Master's thesis

NTNU
Norwegian University of Science and Technology
Faculty of Information Technology and Electrical Engineering
Department of Electric Power Engineering

Mikkel Heiene

Thermal Design of Solid-State Circuit Breakers for MVDC Grids

Design and improvement for performance and cooling of solid-state circuit breakers for MVDC applications

Master's thesis in Master of Energy and Environmental Engineering
Supervisor: Dimosthenis Peftitsis
June 2019

NTNU
Norwegian University of Science and Technology

Mikkel Heiene

Thermal Design of Solid-State Circuit Breakers for MVDC Grids

Design and improvement for performance and cooling of solid-state circuit breakers for MVDC applications

Master's thesis in Master of Energy and Environmental Engineering
Supervisor: Dimosthenis Peftitsis
June 2019

Norwegian University of Science and Technology
Faculty of Information Technology and Electrical Engineering
Department of Electric Power Engineering

Abstract

This master thesis is part of a degree of Master of Technology in Electric Power Engineering and Smart Grids at Norwegian University of Science and Technology.

Design and optimization of a MVDC circuit breaker is a critical stage in implementing MVDC grids for future power systems. An important part of this process is the thermal design. Solid-state circuit breakers suffer from high conduction losses and subsequently heat generation, which must be efficiently dissipated to the environment.

The purpose of this paper is to investigate the thermal behaviour of the breaker and the relevant factors in electrical operation, along with an analysis of current cooling systems. This is done through an overview over current research on the subject, along with MATLAB/Simulink simulations. Based on a literature study, the current interrupting solid-state circuit breaker is found to be the most promising solution. The superior performance of the Insulated Gate-Commutated Thyristor (IGCT) is shown from a comparative study of the investigated devices under different system operating conditions. The analysis of thermal management considers liquid cooling systems to be the most promising concept, while forced air cooling may be beneficial for certain applications.

Table of Contents

Preface i

Table of Contents iv

1 Introduction 1

2 Motivation 3
2.1 Advantages and Challenges of MVDC Systems . . . 3
2.2 Current and Proposed Applications . . . 4

3 Theory 5
3.1 Fault Characteristics in MVDC Grids . . . 5
3.2 Protection Schemes . . . 6
3.3 Proposed MVDC Circuit Breaker Designs . . . 6
3.3.1 Mechanical Circuit Breakers . . . 7
3.3.2 Hybrid Circuit Breakers . . . 8
3.3.3 Solid-State Circuit Breakers . . . 9
3.3.4 Summary of MVDC Circuit Breaker Designs . . . 12
3.4 High Power Semiconductor Devices . . . 13
3.4.1 Device Properties of Interest . . . 13
3.4.2 Insulated Gate Bipolar Transistor . . . 15
3.4.3 Integrated Gate-Commutated Thyristor . . . 16
3.4.4 Bi-Mode Integrated Gate Transistor . . . 19
3.4.5 Other Proposed Devices . . . 20
3.5 Thermal Management of Solid-State Circuit Breaker . . . 22
3.5.1 Basic Thermodynamic Theory . . . 23
3.5.2 Thermal Behaviour of Power Electronic Devices . . . 25
3.5.3 Thermal Equivalent Circuit Models . . . 26
3.5.4 Cooling System . . . 28

4 Design of Solid-State Circuit Breaker **33**
4.1 Design System . . . 33
4.1.1 Electrical Model . . . 33
4.1.2 Thermal Model . . . 35
4.2 Design Considerations and Goals . . . 36
4.3 Passive Component Design . . . 37
4.3.1 Current Limiting Inductor . . . 37
4.3.2 Snubber Capacitor . . . 38
4.3.3 Snubber Resistance . . . 39
4.3.4 Metal-Oxide Varistor . . . 40
4.4 Properties of the Circuit Breakers Designs . . . 41

5 Simulations, Results and Discussion **43**
5.1 Base Case Scenario . . . 44
5.2 Comparative Study . . . 45
5.2.1 Case 1: Varying Nominal System Current . . . 45
5.2.2 Case 2: Varying Current and Voltage at Constant Power . . . 47
5.3 Selection of Power Electronic Device . . . 49
5.4 Sensitivity Analysis . . . 49
5.4.1 Case 3: Varying Thermal Resistance . . . 49
5.4.2 Case 4: Varying Ambient Temperature . . . 50
5.4.3 Case 5: Varying Maximum Temperature Restrictions . . . 52
5.5 Thermal Performance of Cooling Systems . . . 53
5.6 Additional Remarks . . . 53
5.6.1 Impact of Junction Temperature on Devices . . . 54
5.6.2 Transient Thermal Response . . . 54
5.6.3 Improved Analysis through FEM Simulations . . . 54

6 Conclusions and Further Work **55**
6.1 Conclusions . . . 55
6.2 Further Work . . . 56

References **59**

Chapter 1

Introduction

Medium Voltage Direct Current (MVDC) systems have gained a lot of momentum in recent years, due to the substantial increase in performance of power electronics, as well as their many beneficial traits compared to Medium Voltage Alternating Current (MVAC) systems. Still, there are some design barriers to achieve full-scale MVDC grids. The main challenge is related to fault handling. Due to the inherently low inductance of a MVDC grid, regular AC circuit breakers do not operate quickly enough to avoid serious damage to connected components, and require a zero-crossing of current, which is not present in a MVDC grid. A fast acting circuit breaker needs to be developed specifically for MVDC applications. Several topologies have been proposed for this purpose, with one of the main categories being the solid-state circuit breaker, which relies on semiconductor devices for fault clearance. This is able to operate quickly and reliably, but suffers from high on-state losses during normal operation of the grid.

The purpose of this paper is to investigate the thermal design of a solid-state circuit breaker for MVDC grid application. The big drawback of the circuit breaker type is the high conduction losses, which in turn complicate the thermal management of the circuit breaker. Different power electronic devices will be analysed for circuit breaker applications, and the specific requirements of cooling systems will be investigated. Additionally, an overview of related aspects of MVDC grids and electrical performance of the circuit breaker will be provided.

The paper is laid out as follows: In chapter 2, an overview of the MVDC systems concept is given, in terms of feasibility and proposed applications. Chapter 3 provides a theoretical background for the later analysis, along with motivations for choices made in the report. The main points of investigation are circuit breaker concepts, high power semiconductor devices and cooling systems. In chapter 4, the design process for a solid-state circuit breaker is explained. Chapter 5 presents the results of simulations, and discusses the findings according to given design goals. Finally, in chapter 6, the conclusions drawn from the analysis are summarized and some suggestions are made for future work.

Chapter 2

Motivation

Ever since Nikola Tesla came out victorious in the so called ”War of the currents”, Alternating Current (AC) has been the backbone of electrical power systems [1]. However in modern times, Direct Current (DC) is gaining in prominence. One side of this evolution is DC driven low voltage household appliances, and electric vehicles. Another side the evolution is the emergence of High Voltage DC (HVDC) for long range power transmission. Other than this, DC is only utilized in specific applications. Recently, a lot of research has gone into Medium Voltage DC (MVDC) grids, because of their many advantages over their AC counterpart.

The purpose of this section is to elaborate on the potentials of MVDC systems. Firstly, some pros and cons will be presented. Secondly, some potential applications of the technology will be given. Lastly, an overview of the current state of the technology is presented.

2.1 Advantages and Challenges of MVDC Systems

There are several good reasons to choose a DC system over an AC system. Some of the most prominent are listed below:

- **Efficiency:** DC cables have lower resistive power losses compared to AC cables of the same power capacity [2][3]. Fore some applications, conversion stages may be eliminated by utilizing MVDC grids [4, 5, 6, 7], further increasing overall system efficiency.

- **Skin effect:** In AC transmission, opposing eddy currents lead to current crowding close to the conductor surface. This effectively reduces cable cross-section, which in turn increases cable resistance [8]. This is not an issue for DC systems, which increases its material usage and efficiency.

- **Reactive compensation:** In AC transmission, lengthy cables lead to a lowered

power factor. This leads to losses, and may necessitate reactive power compensation. This is not an issue for DC systems.

- **Interconnection:** DC eliminates the need for frequency synchronization between AC grids. In addition, a DC system may be favoured in a grid with high penetration of Distributed Energy Resources (DER) [9].
- **Size and weight:** DC systems require smaller transmission corridors for the same power transfer, leading to less environmental impact [10]. In addition, DC eliminates the need for bulky line frequency transformers, relying on more lightweight converters. For marine vessels or traction systems, this would come as a great benefit.

Although there are some noteworthy advantages, there are still some challenges faced today:

- **Fault handling:** DC grids are characterized by the relatively low impedance and no zero-crossing for the current. This leads to rapidly rising fault currents, which can not be cleared by regular MVAC breakers. As of now, there are no commercially available MVDC scale circuit breakers.
- **Standards and regulations:** Apart from some specific applications, such as traction [11] and shipboard systems [12], there is a lack of standards and regulations for MVDC [6].
- **Cost:** Prices of high power semiconductor devices are still high, leading to costly designs [13]. This, however is decreasing rapidly.
- **Cables:** DC cables have different field characteristics, and are prone to charge accumulation at material intersections [14]. As of now, there is still need for development of specifically tailored MVDC cables [15]. Some research has been made in later years into this subject [16, 17].

2.2 Current and Proposed Applications

Without well performing circuit breakers available, the realization of multi-terminal MVDC grids has come to a halt. Still, there are some developments in the field. In late 2017, Siemens introduced it's new MVDC PLUS concept [18], aimed at efficiently bridging AC networks. In addition, RWTH Aachen has constructed a MVDC distribution grid on campus, for research purposes. Rated at 5 kV [19], this grid could provide some valuable insights. However, the only grid protection is AC side circuit breakers [20]. Therefore, a DC side fault would lead to complete shutdown of the grid [15], and could severely damage the freewheeling diodes of the connected converters [21].

In literature, there have been several proposed applications that would benefit from the efficiency, controllability, and other advantages of MVDC. Among these are marine vessel power systems [12, 22, 23], railway traction systems [11, 24], data centers [25], subsea power transfer [17, 26], and collector grids for solar plants [27] and wind farms [13, 28, 29, 30].

Chapter 3

Theory

3.1 Fault Characteristics in MVDC Grids

The severity of a fault in a MVDC system is driven by several factors. For one, the connected power electronic components are sensitive, leading to strict protection requirements. In addition, the low impedance of the line and its connected converters lead to a rapid current rise. This can be shown by equation (3.1), where $\frac{di_L}{dt}$ represents the current rise through the inductor, L represents the total inductance of the system, and V_L will be the applied voltage. In case of a faulted line, the low inductance thus necessitates fast clearance, in order to properly protect sensitive components.

$$V_L = L\frac{di_L}{dt} \tag{3.1}$$

In a practical multi-terminal MVDC grid, a Voltage Source Converter (VSC) Would be the only viable converter type. The Line-Commutated Converter (LCC) is a mature and reliable technology, found in most point-to-point HVDC connections. However, their lacking controllability, as well as requirements for filtering and reactive power compensation, make them unsuited for practical multi-terminal grids [31, 32]. Therefore, only the VSC fault characteristics will be treated here. There are several basic types of VSCs, all with their own drawbacks and advantages. In order to present the basic operation of a VSC during short-circuit, the relatively simple 2-Level VSC (2L-VSC) is chosen.

In general terms, an incident can be divided into three distinct stages. These three stages are shown in **Fig. 3.1**. During stage 1, the fault current is supplied by discharge of the DC-link capacitor. In stage 2, the capacitor is fully discharged, and does not provide any current. Current is then commutated through the freewheeling diodes, and is driven by the cable inductance. In the beginning of this stage, the current through the freewheeling diodes is at its peak, possibly damaging them. Stage 3 is when the transient response of DC-link capacitor and cable inductance has extinguished. Here, the fault current is directly

supplied by the AC-grid, feeding the fault through the freewheeling diodes. The total fault current is a sum of all three phases.

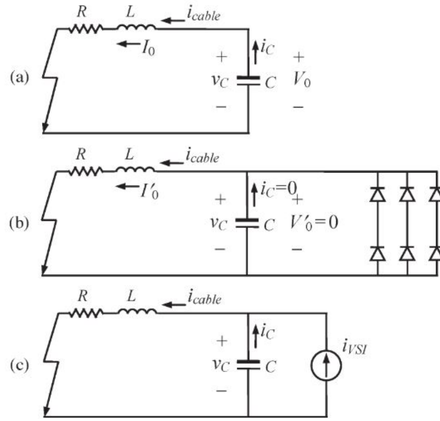

Figure 3.1: Equivalent circuit for 2L-VSC during cable short-circuit fault. (a) Stage 1: Capacitor discharge (b) Stage 2: Diode freewheel (c) Stage 3: Grid current feeding [33]

3.2 Protection Schemes

A significant analysis of protection and coordination is beyond the scope of this paper. Still, the significance and complexity, should be understood.

Fundamentally, network protection needs to adequately follow a set of requirements. These are as follows: Reliability, selectivity, speed, sensitivity and interoperability [34]. These aspects refer to the ability to always follow expected behaviour, the ability to limit protection impact on overall system so that only faulted parts are handled, the speed at which protection reacts, the ability to avoid tripping during regular fluctuations, and the requirements for different components working together.

In a MVDC system, operation speed is of crucial importance, because of the rapid rise of fault currents. Another major issue is the variable operation states of a typical MVDC grid [35, 36]. This requires a high degree of adaptability in protection, leading to more complex and communication-assisted protection schemes [5, 37]. This, of course, is highly dependent on the grid topology.

3.3 Proposed MVDC Circuit Breaker Designs

Currently, there are three main categories of DC circuit breakers, separated by the method of current breaking. These are mechanical, solid-state and hybrid circuit breakers. This paper is focused on the solid-state breaker, the reasons for which will be motivated in this section.

In addition to the three categories mentioned earlier, there are some other methods. These include fuses, which are single-use an thus only viable as back-up protection. Mechanical circuit breakers on AC-side have been proposed [15], but due to long clearance times and lacking selectivity, it should not be used. So-called ”Unit-based” protection has also been proposed [20, 38, 39], relying on breaking capacity of connected power converters and no-load switches. Again, these have limited applicability in MVDC grids, and will not be treated further.

The design criteria for comparison of the breaker concepts, can be boiled down to performance and complexity. In terms of performance, the breaker should minimize breaking time, minimize the maximum fault current in the system, minimize normal conduction losses, and should have satisfactory transient response in no-fault conditions. The on-state losses are also tightly connected to the thermal management requirements, with higher dissipation necessitating more complex and high performing cooling systems. In terms of complexity, the number and size of passive devices should be minimize, as well as the number of separately controlled switching devices. This is directly tied to both reliability and cost. In addition to these, current controllability is an important aspect.

3.3.1 Mechanical Circuit Breakers

Based off the readily available AC circuit breakers, the mechanical DC circuit breakers break current through the use of a mechanical separator switch. In order to force a zero-crossing of the current, an LC resonant circuit is connected. The resonant tank can either be connected directly, which is called passive current injection, or through another switch, which is called active current injection. A basic active resonance mechanical circuit breaker is shown in **Fig. 3.2**.

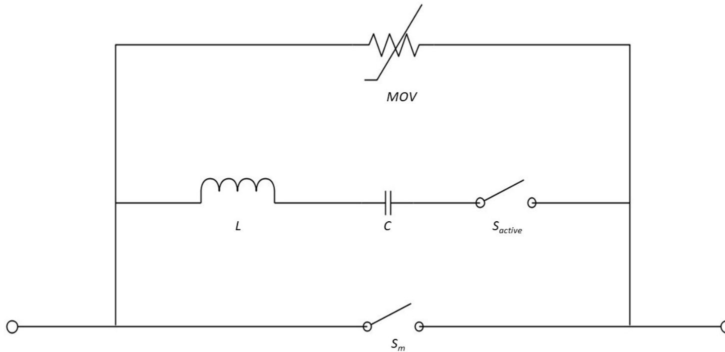

Figure 3.2: Basic mechanical circuit breaker with active resonance current injection

During normal operation, current flows through through the closed mechanical switch, with minimal losses. During a fault, the contacts separate. As the LC branch starts operating, current is forced through zero-crossing, and the fault is cleared. Any residual energy

is then dissipated in the Metal-Oxide Varistor [40].

The low losses during normal operation [37], and the maturity of the technology are the two most prominent advantages of this type of circuit breaker. It is also relatively inexpensive and provides galvanic isolation. The slow operation, however, is the main drawback. In addition, regular maintenance is required [41]. Between the active and passive resonance breaker, the active shows the fastest operation. However, it is still nowhere near the hybrid and solid-state circuit breakers [40].

3.3.2 Hybrid Circuit Breakers

The hybrid circuit breaker is a combination of mechanical and solid-state switching. It was developed as a way of combining the most advantageous properties of the two other breaker types. The basic layout is shown in **Fig. 3.3**.

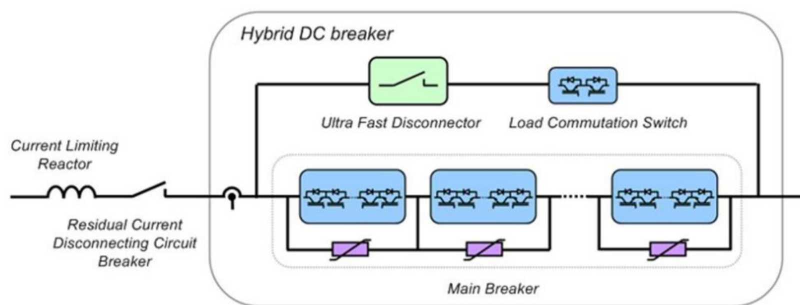

Figure 3.3: Hybrid circuit breaker with series connected solid-state switches for higher voltage rating [42]

During normal operation, the current will flow only through the bypass. In case of a fault, the load commutation switch will open, and and fault current is commutated to the main breaker. The mechanical disconnector opens, and the solid-state branch breaks the current [37, 42]. The limiting factor for speed in this design is the fast disconnector. However, the arc will be handled by the solid-state branch, and so the breaking will be faster than purely mechanical designs [43].

In terms of performance, the hybrid circuit breaker is a compromise between the two other concepts. The mechanical switch leads to the same issues as the mechanical, with longer breaking times and maintenance requirements. Still, when scaling up the design for higher voltages, the on-state losses of the load commutation switch will be significantly lower than for the main switch. Another problem with the hybrid circuit breaker is the complexity. By nature, the number of components, lead to problems of reliability, cost and maintenance [44].

3.3.3 Solid-State Circuit Breakers

The defining characteristic of a solid-state circuit breaker is the reliance of power electronic devices for breaker operations. There are several different topologies proposed for MVDC grids, some of which will be elaborated in this section. These are the current interrupting, current limiting, resistive and resonance topologies. These methods all have normal conduction paths through power electronic devices, but are distinguished by their basic mode of breaking, and their handling of residual inductive energy in the system. Some other solid-state circuit breaker concepts have been proposed, such as a monolithically integrated breaker [45], or several variations of resonance topologies. These will not be elaborated upon, as the main purpose of this section is to identify the most beneficial traits, and thus the most promising concept.

Current Interrupting Topology

The current interrupting circuit breaker is, in its simplest form, a solid-state switching device, with some sort of snubber circuitry, and a Metal Oxide Varistor (MOV). A basic design is shown in **Fig. 3.4**.

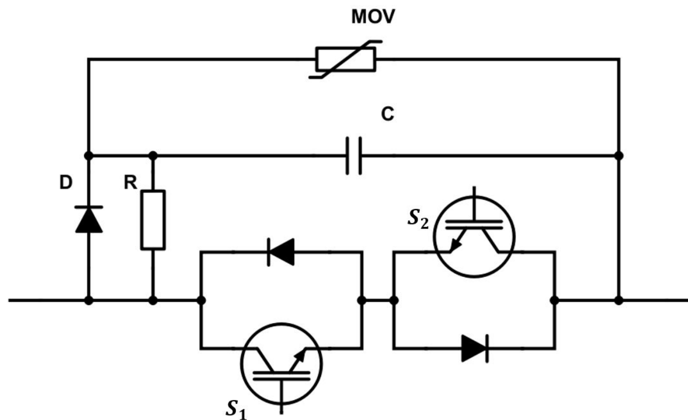

Figure 3.4: Basic bidirectional current interrupting solid-state circuit breaker

During normal operation, the current path goes through the switch, which is in continuous on-state. In case of a fault, the switch will turn off, and current will be commutated to the MOV. After successful switching, the residual energy in the system will be dissipated through the MOV. The purpose of the RCD snubber circuitry is to reduce the overvoltage stresses during turn-off, and in case of series connection, to ensure proper voltage sharing between the devices [46]. In addition, a current limiting inductor is connected in series, in order to limit current rise during fault. The slope limiting inductance should be minimized, in order to avoid additional energy that must be dissipated [47].

The benefits of this topology over the others are mainly in the fast fault clearance [48, 49, 50] and simple design. This concept requires few connected switching devices and separate gate drives, and has the fasted reported fault clearance among the proposed

topologies. Its modular nature also makes it suitable for scaling up. The biggest drawbacks are the relatively high current stresses and on-state losses [51].

Current Limiting Topology

The current limiting circuit breaker is a line-to-line connected breaker with freewheeling paths opening for fault clearance. A basic bidirectional design is shown in **Fig. 3.5**.

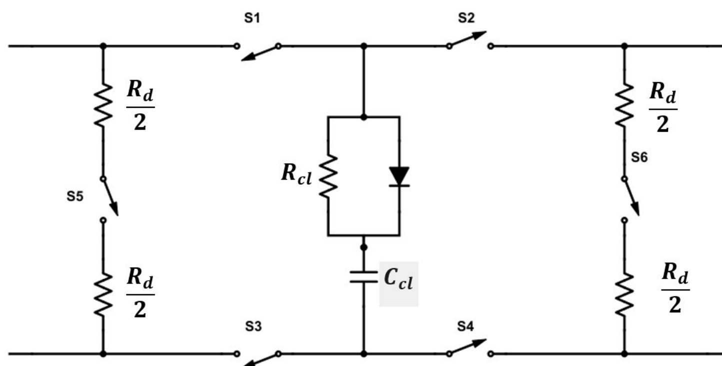

Figure 3.5: Basic bidirectional current limiting solid-state circuit breaker

During normal grid conditions, the power flows through switches S1-S4. In case of a sensed fault, the fault-side series switches are turned of, and current is commutated through the midpoint, which is a clamping circuit. Next, the fault is decoupled through closing of the fault-side parallel switch, S5 or S6. After the fault is decoupled, the residual is dissipated through R_d. The dissipating resistor is subject to a trade-off. Reducing its resistance would lead to faster zero-crossing, it would also reduce its energy dissipation capabilities [39].

In terms of performance, the limiting topology has lower voltage stresses on the devices [52], and the fast operation and optimization of energy dissipation are beneficial characteristics [53]. This gives lower losses, and simpler scaling [51]. Still, the complexity and high sensing demands make it difficult to implement. The high number of components and individual switches make tuning and control problematic, and the extra of current paths and passive components may cause unwanted transient effects. In addition, the packaging and scaling of this design is hard, due to its many components and its basic operation.

Resistive Topology

The operating principle of a resistive circuit breaker is utilizing switching operations in order to emulate a high series resistance during a fault. In **Fig. 3.6**, a basic bidirectional design is shown.

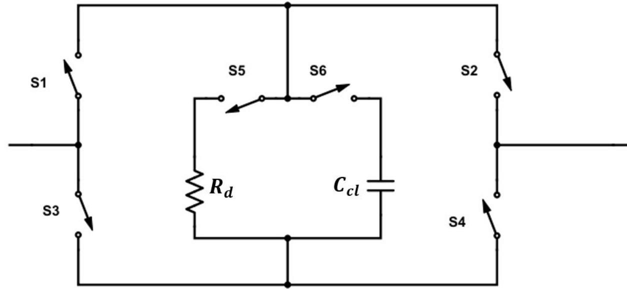

Figure 3.6: Bidirectional resistive solid-state circuit breaker

During normal operation, nominal current is divided between the two parallel branches, with S5 and S6 in off-state. In case of a fault, the clamping capacitor C_{cl} will be charged up until it reaches a set voltage. When this value is reached, switches S5 and S6 turn on, and the capacitor is discharged through the dissipating resistance R_d. When the voltage across C_{cl} falls below a set value, S5 and S6 open again, repeating the cycle. These operations continue until the fault current is reduced to zero.

This concept has some important characteristics to keep in mind. One is that the clamping capacitor has to be pre-charged if the breaker is to operate fast enough. In addition, we have relatively high frequency switching operations, but this will increase the total system energy that must be dissipated in R_d [54].

This topology has several advantages. For one, the switching operations of the midpoint path renders the breaker fully controllable, within certain limits. The parallel paths for current reduces the on-state losses in the switching devices. In addition, the size requirements of passive components are relatively low in this design. This is, however, a highly complex and costly circuit breaker, with a high component count and demanding drive systems. In addition, the system is sensitive to large cable inductances, and the reliance on dissipating capabilities of a resistor could prove problematic [51].

Resonance Topology

There are several proposed topologies for resonance solid-state circuit breakers. All of these are based on the principle of RLC-branches forcing fault current to zero during faulted conditions. After breaking, residual energy will be dissipated in the resonant elements. This mode of operation has the potential of automatic operation, meaning that sensing and coordination can be made redundant. Another consequence is that fully controllable switches are not necessary. A thyristor, for example would naturally turn off once the current drops to zero-crossing. Either way, a cheaper and more optimized device can be utilized, as turn-off capability is not an issue. The resonance topology thus have the possibility of significantly lower on-state losses, and control is relatively simple.

Resonance solid-state circuit breaker can be divided into three different types, each categorized by their activation method. We have the gate-commutated [55, 56], the coupled inductor [57], and the Z-Source [58, 59].

Although these topologies show significant advantages, there are some drawbacks. The reliance on passive elements lead to a bulky design, and response to changes in the connected grid are hard to predict. This may cause false tripping and transient disturbances caused by the breaker. For MVDC grids in particular, the lack of control may cause trouble.

3.3.4 Summary of MVDC Circuit Breaker Designs

The design criteria for a MVDC circuit breaker were identified at the beginning of this section. These include short breaking time, low maximum fault current in the system, low conduction losses, good transient response to variable grid states and occurrences, and minimum complexity.

Between the three overall breaker methodologies, the solid-state circuit breaker is considered to be the best choice for MVDC applications. The mechanical and hybrid solutions have some advantages in terms of conduction losses. The mechanical breaker, in particular, has the benefit of technological maturity and cost. The hybrid breaker operates similarly to the solid-state solution, but with considerably lower losses. Still, the benefits are outweighed by the slow operation times and inability to sufficiently dampen fault currents. In [24], a performance simulation of the methods was done for a hypothetical 15 kV grid rated at 1.5 kA nominal current. The results of this study are repeated in **Tab. 3.1**. This shows that a solid-state circuit breaker is the only viable solution with current technology. The main challenge, namely power losses, is also clear.

Circuit breaker type	**Fault Current [kA]**	**Clearance Time [ms]**	**Residual Energy Dissipation [kJ]**	**Power losses [kW]**
Mechanical	51.1	15	645	0.23
Hybrid	19.5	3.4	246	8.3
Solid-State	3.18	0.6	1.4	30

Table 3.1: Performance of circuit breaker types [24].

From the different solid-state circuit breakers, the current-interrupting topology is considered to be the best option. It has a simpler, less bulky, and more controllable design and operation compared to the resistive and current limiting topologies. The resonance topology has a simpler control system, but as previously stated, the limited control can prove problematic. In terms of operation speed, several cases have been reported in literature, and an overview comparison was made in [51]. The reported time intervals are replicated in **Fig. 3.2**. From this, it can be concluded that the operation speed of the interrupting topology is substantially faster than the others.

In summary, the current interrupting solid-state circuit breaker is found to be the most promising concept for MVDC applications. This is also technology that is likely to have the most significant improvements through the continuing evolution of power electronic devices.

Topology	Documented Current Limiting Time [μs]
Current Interrupting	0.8 – 70
Current Limiting	150 – 2500
Resistive	20 – 900
Resonance	200 – 4000

Table 3.2: Operation speed of solid-state circuit breaker topologies [51]

3.4 High Power Semiconductor Devices

For a good design of a solid-state circuit breaker, the performance of the semiconductor devices are of crucial importance. These are central to both the power transmission efficiency during normal operation, and the fault handling capabilities. Power electronic devices have been under heavy development in recent decades. This has given a surge in new types of devices, optimized performance of existing devices, new applications and even utilizing new materials. Commercial applications are mostly in converters, and so most of the devices are also optimized for this purpose. For power electronic devices in circuit breakers, the design goals are slightly different. Mainly, the switching frequency and associated losses are of high importance in converter applications. In the future, some trade-offs should be considered for breaker applications.

Some distinctions can be made between the different available devices. One such distinction is between majority carrier devices and minority carrier devices. This refers to the method of conduction and blocking. Majority carrier devices rely on the effect of an externally applied field to create a conducting path. This leads to the possibility of faster switching. Minority carrier devices rely on both minority and majority charges. They are operated through internal charge diffusion, and thus pn-junctions, for conduction and blocking operations. The minority carrier devices are capable of higher charge density, which gives them better on-state performance. Another distinction is the packaging. For high power applications, devices are sold either as individual modules, or press-pack devices. These differ somewhat from each other in cost and mechanical mounting. Mechanical mounting is important when it comes to connection and the use of cooling systems.

The purpose of this section is to identify which properties are of interest for devices used in a solid-state circuit breakers, and present currently available devices. In addition, some attention will be given to proposed devices that may be relevant in the foreseeable future.

3.4.1 Device Properties of Interest

As previously stated, devices for circuit breakers have slightly different requirements compared to converter applications. In a solid-state circuit breaker, the devices are continuously conducting during normal operation, and switching operations only occur during a fault. Behaviour and operation of individual devices will be discussed later later. The relevant properties of such devices are listed below:

- **Maximum rated blocking voltage:** This is property of material and geometry. Exceeding this value leads to critically high electric field within the device, and may lead to breakdown and device failure.
- **Maximum rated current turn-off capability:** This value defines the highest current at which the device is able to reliably perform a switching operation. Exceeding this value may lead to turn-off failure, which would be especially dangerous in circuit breakers.
- **Maximum rated operating current:** Often given at given junction temperatures, this value dictates the continuous current capability of the device. Exceeding this value would over-heat the device, risking component failure.
- **Conduction losses:** Energy dissipation during normal operation is dictated by the two components of the on-state losses. These are given by a combination of a constant voltage drop across internal pn-junctions of the device, and a resistive element through the terminals and the semiconductor material. The total heat dissipation losses then become as shown in equation (3.2), where V_0 is the built-in voltage drop, I_{AV} is the average current running through the device, r_T is the ohmic component, and I_{RMS} is the RMS current running through the device.

  $$P_{on} = V_0 \cdot I_{D(AV)} + r_T \cdot I_{D(RMS)}^2 \tag{3.2}$$

  For DC application, there is no meaningful distinction in terms of the current, and the equation is simplified into equation (3.3).

  $$P_{on,DC} = (V_0 + r_T \cdot I_D) \cdot I_D \tag{3.3}$$

  The on-state voltage mechanisms are different for each type of device. However, the general representations used in the previous equations hold true. V_0 is a current-independent voltage drop that is required to keep the device conducting. r_T is a representation of all resistive losses from the operation. These include both resistive losses as charges move through the device material, as well as resistance in connectors and packaging.

  On-state losses is a major complicating factor for solid-state circuit breakers. For current devices, these losses are high enough that they significantly reduce the overall system efficiency. In addition, all the generated heat needs to be conducted away from the device, which means that better performance is required from the cooling system.
- **Robustness facing high rate of current and voltage rise:** For various reasons, devices may have trouble when being exposed to high rates of rise in current or voltage. These are expected to occur in a MVDC circuit breaker, so the devices must be protected. High sensitivity to these conditions would necessitate bigger capacative snubber circuits and current limiting inductors.

- **Ease of parallel and series connection:** Although the voltage levels of MVDC grids are not properly defined, application specific cases have identified ranging from 1 kV to several tens of kilovolts [22, 26, 29, 60, 61, 62], with some researchers even going as high as 70 kV [63]. As current silicon-based devices are limited to a breakdown voltage of 6.5 kV, series connection would be required to handle higher voltages. In addition, the rated current of such systems may be expected to exceed the current ratings of a single device, thus necessitating parallel connections. However, scaling up designs is not a matter of simply increasing voltage and current capabilities. If not properly designed, small variations in conditions may cause a mismatch of voltage or current between the devices. This would give unpredictable designs, and could stress components beyond their capabilities. For voltage balancing, RC-, or RCD-snubbers are common [64, 65]. For voltage-controlled devices, driver circuits can also be specifically designed voltage sharing [66]. In order to properly operate parallel connected devices, a positive temperature coefficient is a simple and reliable solution. The temperature coefficient refers to the thermal dependency of conduction. A positive value ensures that current sharing between paralleled devices are self-regulating [67]. Alternatively, the gate driver could be adapted for this purpose. but this would increase the complexity significantly.

- **Thermal conduction capabilities:** As the continuous conduction generates heat, the semiconductor devices need to be able to properly dissipate this heat into the environment. External cooling systems play a major role in this, of course, but the thermal impedance of the device itself is also of great importance. In this, we have both the thermal conductance and the heat capacity. Thermal behaviour power electronic devices will be elaborated upon later in this chapter.

3.4.2 Insulated Gate Bipolar Transistor

The Integrated Bipolar Transistor (IGBT) is a gate-voltage controlled, minority-carrier device. Topologically, it is a thyristor with a Metal-Oxide-Semiconductor (MOS) gate. However, the thyristor action is considered a parasitic effect, and must be suppressed. In operation, the IGBT is closer to an interconnected Bipolar Junction Transistor and Metal-Oxide-Semiconductor Field-Effect Transistor (MOSFET). In **Fig. 3.7**, a commercial press-pack IGBT from ABB is shown.

Figure 3.7: Commercial StakPak IGBT Module [68]

The IGBT has been around for a long time, and has proven its merits for high power applications. Current IGBTs can reach breakdown voltages as high as 6.5 kV. However this is at the cost of conduction losses and current capabilities [43]. The high power density, as well as relatively simple series and parallel connection are important characteristics in circuit breaker application. Press-pack IGBTs also have the advantage of short-circuit failure mode [69], good thermal cycling performance, and the possibility of double-sided cooling. Press-pack devices are thus most suited for use in solid-state circuit breakers.

Electrical Properties

In conducting mode mode, the IGBT has several loss mechanisms. There is a constant voltage drop from biasing pn-junctions in the device, as well as a resistive component from charges flowing through the MOS-channel and the drift region.

When turning off, the device voltage is lowered below its threshold, which removes the inversion layer required for operation. an initial time delay occurs, before the voltage starts rising. The MOSFET-section shuts down, depleting the major current component. Lastly, a trailing current caused by stored charge remains, which is depleted when all charges have recombined.

For higher voltage and current capabilities of the circuit breaker, series and parallel connection of several IGBT devices may be necessary. IGBT press-pack devices have a strong positive temperature coefficient, making parallel connections simple. For series connection, dynamic voltage sharing can be troublesome. The fast switching transients of IGBTs lead to passive snubber circuits not being sufficient [70]. However, IGBTs have the advantage of being the only self-commutated devices that can control its switching dynamics with a gate driver. Because of this, an active gate driver circuit can be used to ensure stable dynamic voltage sharing in series connection. This somewhat complicates the gate driver circuit design, but it has achieved significant results in studies [71].

3.4.3 Integrated Gate-Commutated Thyristor

The Integrated Gate-Commutated Thyristor (IGCT) is a minority-carrier device, developed in the late 90s for high power applications [64]. It is an evolution of fully controllable switches based on thyristor technology. Thyristors are currently in widespread use

for high voltage systems, because of their low voltage drop, and their high voltage and current capabilities. However, turn-off requires a natural zero-crossing of the current. The Gate Turn-Off thyristor (GTO) is an iteration of the standard thyristor, achieving turn-off capability. This is done by introducing a pn-junction at the gate connection, through a local difference in doping concentration. This makes the GTO an efficient high power device for applications that require full controllability. Still, there are some issues with this design. The high storage time are one drawback, more so for switching applications, where this severely limits the maximum switching frequency. Another drawback is requiring a negative gate current as high as between 1/5 and 1/3 of anode current to turn off [72]. In addition, the inhomogeneous switching transients leads to high dv/dt and di/dt snubber requirements [73]. The IGCT was developed in order to counter some of these problems. **Fig. 3.8** shows an example of a commercial IGCT device.

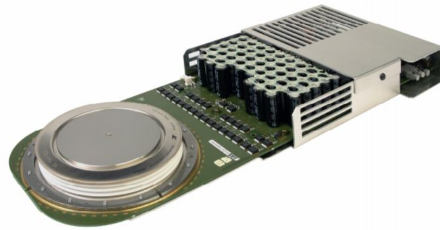

Figure 3.8: Commercial IGCT Module [74]

As a high power device, all commercial IGCT are packaged as press-pack devices. This enables double-sided cooling, short-circuit failure mode and simple stacking. A stack would be mounted with relatively high force, and with interleaving cooling system modules. The heat sinks also serve as electrical connection between the IGCT terminals.

The transparent anode and punch through structure introduced with the IGCT [75] lead to a lower gate power requirement [76], as well as lower conduction losses [77]. The buffer layer gives an almost constant electrical field in the blocking pn-layer, which means that a high blocking voltage can be achieved with a thinner device, again improving losses. The integrated low-inductance drive circuit enables a snubberless design and significantly lower storage time, through hard switching of the device [78, 79].

IGCT Device Variations

The development of the IGCT has lead to three different types of devices. These are the Asymmetric IGCT (A-IGCT), the Reverse Conducting IGCT (RC-IGCT), and the Reverse Blocking IGCT (RB-IGCT). The different devices are are presented in **Fig. 3.9**.

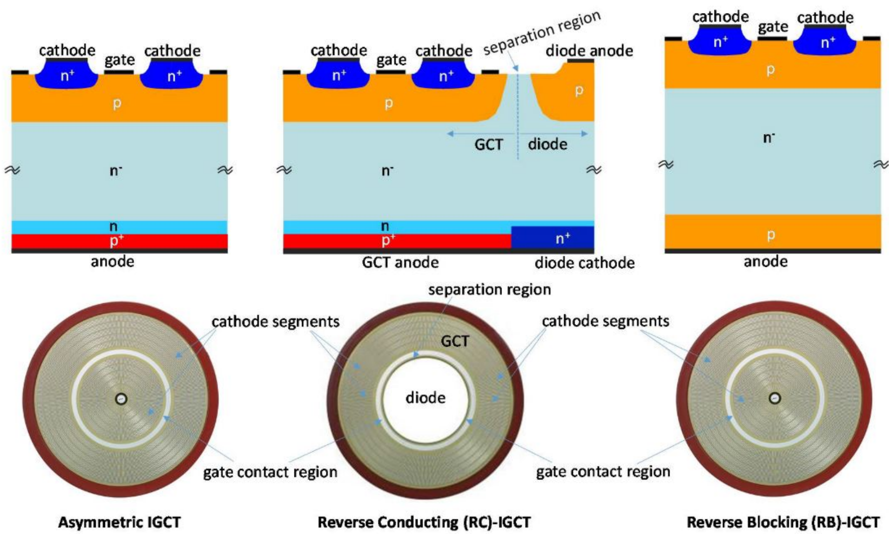

Figure 3.9: Cross-sections and overview of IGCT devices [80]

In terms of power density, the A-IGCT is the most efficient. However, it can only conduct and block in forward direction. For reverse blocking, it will require a diode in series, and in order to achieve bi-directional operation, another anti-parallel branch would be required. The RC-IGCT can conduct in both directions, but only block forward voltage. For bi-directional operation, a back-to-back configuration of two devices is needed. This is the most compact design of the three, as it integrates a diode and a GCT in one device. Unfortunately, this leads to low waver utilization, as there is less space available for conduction. Because of this, available RC-IGCTs have lower current ratings than A-IGCTs. The RB-IGCT is not commercially available yet. It can block current in both directions, but only conduct forward current. For bi-directional operation, two devices are connected in anti-parallel. As seen in **Fig. 3.9**, the wafer is thicker, leading to more ohmic losses during conduction. However, only one device is conducting at a given time, which means lower losses [81, 82].

Electrical Properties

When turning on, the IGCT latches on to a high gate-current pulse, and stays on thanks to the regenerative process of the thyristor action. During normal on-state, the IGCT operates in a similar fashion to a thyristor. Thanks to current injection from two internal BJT-equivalents, the space charge density is very high [83]. Conduction losses are relatively low, being driven by voltage drops across the internal junctions, and a field driven voltage drop in the drift region.

When turning off, the gate-cathode junction is reverse-biased to allow current blocking. The device behaves like an open-base PNP-transistor, generating similar losses as an IGBT. Comparing to a GTO, the IGCT has the advantage of hard-switched turn-off, as current is rapidly commutated away from the cathode and through the gate. This reduces

the time of inherently unstable transition from thyristor mode to transistor mode. A stable opreation can thus be achieved even without snubber circuitry.

In terms of voltage sharing, series connection of the IGCT can be an issue, due to parameter spread, and so series connected IGCTs should always be snubbered. Turn-off is the most critical in this situation, as the turn-on waveforms are more predictable. Thankfully, the use of RC- and RCD-snubbers are well established for IGCT devices. Being a current-controlled device and having a pre-packaged gate driver, the series connection cannot be improved further as with IGBT active gate drivers. In case of parallel connection, all commercial IGCTs have a strong positive temperature coefficient, making current-sharing feasible.

3.4.4 Bi-Mode Integrated Gate Transistor

The Bi-Mode Integrated Gate Transistor (BIGT) is a recent development, which integrates an IGBT and a Reverse Conducting IGBT (RC-IGBT) on one chip. The basic structure of this device is shown **Fig. 3.10**. This figure shows the hybrid structure of the BIGT, as well as the miniaturized MOS-cells.

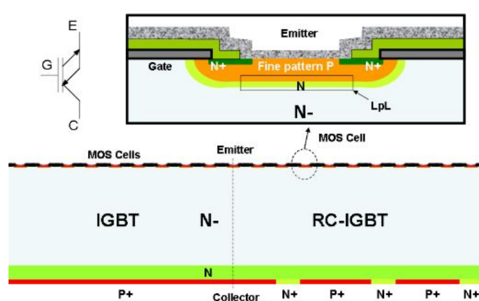

Figure 3.10: Basic structure and proposed circuit symbol for a BIGT device [84]

A significant advantage of the BIGT structure is that the full silicone volume can be used independently of whether the device is in IGBT mode or diode mode. This has a positive impact on total losses and wafer utilization, as well as thermal management. The BIGT has also shown better performance in terms of Short-Circuit Safe Operating Area (SCSOA) and voltage handling capability [85]. In case of higher power requirements, a strong positive temperature coefficient has been shown [84]. Along with the previously discussed series connection properties of the traditional IGBT, the BIGT should be relatively simple to implement in a circuit breaker with multiple devices.

A remarkable feature of the BIGT is related to its transient behaviour. For traditional IGBTs, soft transient design is a matter optimization process seeking to match properties of the IGBT and the anti-parallel diode. In experiments, the BIGT has shown inherent soft switching transients, which has been attributed to an effect termed field charge extraction [86]. This effect occurs in the MOSFET section, as the field can extract additional cathode carriers to aid in soft recovery [87].

In terms of electrical properties and behaviour, the BIGT can be analysed as an IGBT device, as its basic operation remains unchanged.

3.4.5 Other Proposed Devices

In addition to the IGBT, IGCT and BIGT, there are several other proposed devices for solid-state circuit breaker application. This includes different topological innovations, as well as Wide-Bandgap (WBG) devices. The devices in question are either not commercially available, or have not reached the required voltage and current ratings to be considered as viable alternatives.

Bi-Mode Gate-Commutated Thyristor

The Bi-Mode Gate-Commutated Thyristor (BGCT), is a conceptual iteration on the RC-IGCT design. The idea of integrating GCT and diode on the same wafer is similar, however, the BGCT solves this through interleaved sections, as shown in **Fig. 3.11**.

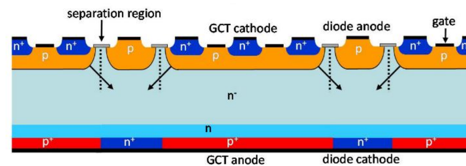

Figure 3.11: Schematic structure of a Bi-mode Gate-Commutated Thyristor [88]

This design has a vastly improved wafer utilization compared to the classic RC-IGCT. This comes from the increased effective area, as current flow is not bound to the respective GCT and diode segments. This gives the device higher current capability and lower conduction losses, as well as improved plasma distribution giving the device lower thermal resistance and better dynamic thermal behaviour [88, 89].

This device is still in development, with no commercial modules. The concept could however be useful in the future as an efficient integration of IGCT and diode into a single structure.

Emitter Turn-Off Thyristor

The Emitter Turn-Off Thyristor (ETO) MOS-GTO hybrid design, with voltage controlled turn-off [90]. The equivalent circuit diagram of this device is shown in **Fig. 3.12**. The two MOS switches, Q_E and Q_G are connected in series with respectively the emitter terminal and the gate terminal of the GTO. During normal conduction, Q_E is on, while Q_G is off. When turning off the device, the cathode current path is blocked by switching off Q_E, and current is commutated to the gate path. It should be noted that neither of the MOS-switches experience a high voltage stress at any point in operation [91].

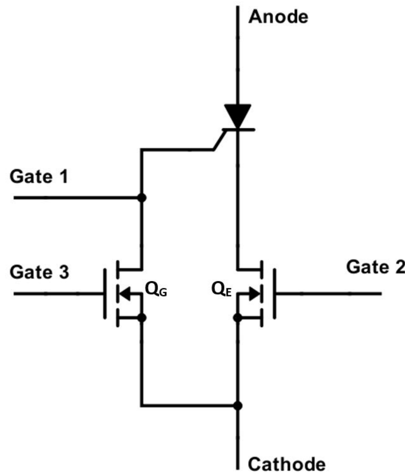

Figure 3.12: ETO equivalent circuit diagram

Several researchers have proposed the ETO for use in MVDC solid-state circuit breakers [48, 72, 91, 92, 93]. The reported advantages are among others an increased turn-off speed, higher maximum turn-off current capability, and a wider Reverse Bias Safe Operating Area (RBSOA). These benefits are caused by the hard driven turn-off process at unity-gain [67]. In comparison to other controllable thyristor-based devices, the ETO also have lower gate power [67]. Additionally, the internal current sensing capability could possibly simplify the overall circuit breaker design.

As of now, the ETO is still in not commercially available, even though it was introduced as early as 1998 [90]. There is still some development required, and some issues with current ETO designs. Most notably, there are some uncertainties in its ability to short-circuit in case of component failure. This is not acceptable for high power press-pack devices.

Super Gate Turn-Off Thyristor

The Super Gate Turn-Off Thyristor (SGTO) is a design patented by the Silicon Power Corporation, with the purpose of an improved GTO design. The production process is altered by implementing planar integrated circuit, which gives about 3 000 times higher cell density compared to standard GTOs [94]. This substantially improves the on-state voltage drop. The thinner device also has a much lower switching time [95, 96]. The SGTO also has good thermal conductivity for the full packaged device, although double-sided cooling is ineffective with current designs [97].

Although the SGTO has several beneficial traits for use in MVDC circuit breakers, with some proposed applications in litterature [94, 98, 99], there are no commercially available devices, and so they will not be studied further.

Wide-Bandgap Seimconductor Devices

A new development in the field of semiconductor materials is the emergence of WBG materials for power electronic devices, such as Silicon Carbide (SiC) and Gallium Nitride (GaN). In the recent years, these have been under substantial research, and have found many applications in power electronic devices. Of these, several have been proposed for use in circuit breaker applications. Some of these are the SiC MOSFET [100, 101], SiC Junction Field-Effect Transistor (JFET) [45, 100, 101, 102], SiC ETO [93] and GaN HEMT [103, 102].

WBG materials differ from traditional Silicon (Si) in their basic quantum mechanical properties. The energy difference between the conductance and valence bands is bigger, at 1.12 eV for Si, 3.23 eV for 4H-SiC, and 3.4 eV for GaN. In semiconductor device design, this wide bandgap has some important benefits. The carrier concentration can be made higher, which enables better charge mobility and thus improves the material conductivity. The wide bandgap also leads to a higher breakdown field, which means that smaller devices can block higher voltages. This also reduces minority charge storage, which improves switching performance [77].

Thermal characteristics are also an benefit of WBG devices, especially for SiC. WBG devices are capable of operating at higher temperatures, reducing cooling needs. The big advantage of SiC comes from its thermal conductivity. Regular crystalline Si has a thermal conductivity of $\lambda_{Si} = 1.48 cm^{-1} {}^{\circ}C^{-1}$, and GaN is reported to have a thermal conductivity of $\lambda_{GaN} = 1.3 cm^{-1} {}^{\circ}C^{-1}$. SiC has a higher conductivity, at $\lambda_{SiC} = 3,7 cm^{-1} {}^{\circ}C^{-1}$. This implies that SiC devices will be far better suited to efficiently dissipate generated heat, and can have a higher power density.

Despite the beneficial material properties, there are no currently available devices for the current and voltage capabilities required for a well-performing solid-state circuit breaker. At this point in development, high manufacturing costs and uncertainties in threshold voltage levels represent major barriers [104]. Depending on the type of device, there are several barriers in development that need to be overcome before WBG devices can be applied in MVDC circuit breakers. Therefore, no more focus will be given to WBG devices in this paper.

3.5 Thermal Management of Solid-State Circuit Breaker

Because of the substantial conduction losses found in a current interrupting circuit breaker, the thermal management needs to be properly integrated in any real design process. Thermodynamic behaviour and the effect of heating on device operation are intrinsically complex, and a deep understanding of the topic is needed for a functional design.

The purpose of this section is to substantiate the relevant characteristics as well as presenting the basic methodologies of cooling systems. Firstly, a summary of thermodynamic mechanisms will be made. Then some application specifics for power electronics will be analyzed. Next, the common methods of thermal management are presented.

3.5.1 Basic Thermodynamic Theory

In thermodynamic theory, there are three mechanisms stated as the different modes of heat transfer; conduction, convection and radiation. In order to grasp the theory behind thermal management of semiconductor devices, one has to understand their underlying mechanisms. The three modes of heat transfer will be treated in this section.

Thermal Conduction

Thermal conduction is the mechanism of heat transfer through the collision or vibrations of particles at a microscopic level. These interactions give rise to an exchange of kinetic energy between particles, and thus alters the temperature distribution in the medium.

For modelling heat transfer through conduction, we have Fourier's law of heat conduction. This is given in its differential form as equation (3.4). **q** is the heat flux density, k is the thermal conductivity of the material, and ∇T is the temperature gradient.

$$\mathbf{q} = -k \cdot \nabla T \tag{3.4}$$

In order to visualize this, one can imagine a plane between a hot medium and a cold medium. This is relevant for solid-state devices, as they have different layers within. If we assume a simplified case with temperature T_1 in the hot medium, and a temperature T_2 at the cold side, along with a contact surface A_c and a thickness Δx, we can calculate the rate of heat conduction through the plane layer, $\dot{Q}_{cond}$ as in equation (3.5).

$$\dot{Q}_{cond} = k \cdot A_s \cdot \frac{T_1 - T_2}{x_1 - x_2} = k \cdot A_c \cdot \frac{\Delta T}{\Delta x} \tag{3.5}$$

This simplified equation shows us the relevant factors in thermal design of devices. For improved junction-to-case heat transfer, one can utilize materials with better conductivity, increase the ratio between contact surface and thickness, or increase the temperature gradient. In a three dimensional object with the complexity of a power electronic device, this simplification is lacking. It is, however, a good conceptual description of conduction cooling. In a practical application, conductive heat transfer is the defining mechanism of heat transfer between junction and heat sink.

Convective Heat Transfer

Convection heat transfer is caused by the bulk movement of molecules in fluids. This is the dominating mechanism when it comes to transferring heat from an extrusion into the ambient. This is an innately complex mechanism, with several driving factors. For the purposes of this paper, however, we can limit ourselves to the processes of natural convection and forced convection. It should be noted that methods involving phase change, are considered as convective mechanisms.

Natural convection is driven by the temperature dependency of density, which in turn causes hot air to rise up, in effect cooling the boundary layer between material surface

and fluid. This is the driving factor for natural convection cooling systems, where passive extrusions transfer heat from case to ambient.

Forced convection is the process of fluid movement by external forces. This is a common method of increasing cooling system efficiency and controllability. In forced air cooling and liquid cooling, this is the dominating mechanism. Here, the speed of fluid flow has a crucial impact on heat transfer.

Mathematically, convection is an incredibly complex problem. In simple cases, however, one can calculate the rate of convective heat transfer $\dot{Q}_{conv}$ through equation (3.6). Here, h is the convective heat transfer coefficient, A_s is the effective surface area, T_s is the temperature at the interior of the material, close to the surface. T_{amb} is the temperature of the environment sufficiently far away from the surface.

$$\dot{Q}_{conv} = h \cdot A_s \cdot (T_s - T_{amb}) \tag{3.6}$$

In order to control the rate of heat transfer from heat sink to environment, this model presents some tools. First off, the coefficient h can be manipulated. This can be done either by using different fluids, or forcing convection. A summary of typical heat transfer coefficients of different methods are given in **Tab. 3.3**. As the table shows, the differences are substantial. The heat transfer coefficient is also highly dependant on the bulk fluid velocity. Secondly, the surface geometry can be altered, in order to either increase effective surface area, or to change the nature of fluid flow. Lastly, the temperature difference can be increased, usually by decreasing ambient temperature by some means.

Convection method	**h** $[W/(m^2 °C)]$
Natural, gasses	2 – 25
Natural, liquids	10 – 1000
Forced, gasses	25 – 250
Forced, liquids	50 – 20 000
Boiling/Condensation	2 500 – 100 000

Table 3.3: Typical values for convective heat transfer coefficients of various mediums

Thermal Radiation

Radiative heat transfer is driven by the emission of electromagnetic waves from thermal motion of particles in a medium. This mechanism is unique in the sense that it does not need the presence of another interacting medium, and it occurs in all matter at a temperature above absolute zero.

The formula governing thermal radiative heat emission $\dot{Q}_{rad}$ is the Stephan-Boltzmann law, shown in equation (3.7). Here, ϵ is emissivity, a material property with a value between 0, where no thermal radiation occurs, and 1, where the theoretical maximum is. This maximum is called black body radiation. σ is the Stefan-Boltzmann constant, defined as $\sigma = 5.670 \cdot 10^{-8} W m^{-1} °C^{-4}$.

$$\dot{Q}_{rad} = \epsilon \cdot \sigma \cdot A_s^4 \cdot T_s^4 \tag{3.7}$$

The Stefan-Boltzmann law shows that the heat emission increases with a power of four for increased surface area and temperature. At operating conditions for semiconductors, however, the contribution is normally negligible compared to conductive and convective components [105]. In situations where the increased radiative heat emission is beneficial, the surface material can be altered. Painting the surface with matte black finish, witch has a substantially higher emissivity than polished metal is a common method in such cases. Other methods include anodized aluminum or oxidized copper heat sinks.

3.5.2 Thermal Behaviour of Power Electronic Devices

As previously stated, the main contributor to heat generation in a solid-state circuit breaker will be the on-state losses of the semiconductor devices. The heat will emanate from the junction of the devices, and will have to be dissipated into the environment through a heat sink.

Heat transfer from junction to heat sink is dependant on the devices heat transfer characteristics, i.e. thermal conductivity and heat capacity. The thermal conductivity is a defining property of thermal resistance, is described by the equations (3.8) and (3.9). In these equations, R_{th} is the thermal resistance between two points, d and A are respectively the distance and cross-sectional area of the medium, λ is the thermal conductivity of the material, Q is the heat flow, and ΔT is the temperature difference between two points in the medium.

$$R_{th} = \frac{d}{\lambda A} \quad [^{\circ}C/W] \tag{3.8}$$

From this equation, it is clear that there is a linear dependency of geometrical properties and conductivity. One way to improve thermal properties of a device is to tweak its geometry. Another can be to use other semiconductor materials. With the numbers presented in chapter 3.4.5, a SiC device would have more than three times lower thermal resistance as a Si device of same dimensions.

$$Q = \frac{\Delta T}{R_{th}} \quad [W] \tag{3.9}$$

Equation (3.9) shows how the heat flow between two points is dependant of the thermal resistance and the temperature difference. From this, we can deduct that the ambient temperature can have a significant impact on cooling requirements.

In transient analysis, the heat capacity of a device is also important to take into account. This is a measure of how much thermal energy is required for an incremental increase in the temperature of the material. The heat capacity is obtained by equation (3.10), where

c_p is the specific heat capacity, i.e. per unit mass, and ρ is the volumetric mass density of the material.

$$C_{th} = c_p \cdot \rho \cdot d \cdot A \quad [J/^{\circ}C] \tag{3.10}$$

In thermal analysis of a power electronic device, the heat capacity is a measure of how long it takes for the device to heat up when applied a certain amount of heat. This will be elaborated in the section concerning thermal models.

During operation, the cooling requirements are not only related to a maximum operating temperature. The performance of power electronic devices have a strong temperature dependency. Most press-pack devices have a positive temperature coefficient, which means the on-state voltage drop would be higher at elevated temperatures. The turn-off capability would also be reduced. When designing a cooling system, one has to either accept poorer electrical performance, or tighten the constraints on the cooling system.

Mounting Considerations

When connecting the heat sink and power electronic component, one can not assume that heat flows unimpeded between the two. Both components will have a surface roughness, and depending on mounting they will have a slightly decrease in heat conduction capacity. To counteract this, Thermal Interface Materials (TIM) are often utilized. This can either be a type of grease or a gel, thermally conductive adhesive tape or compound materials, or more advanced materials, such as phase change materials or carbon nanotubes [106, 107].

In press-pack stacks, an uneven or rough surface interface will also lead to resistive losses, decreasing efficiency and generating additional heat. To avoid this effect, a thin coating of conductive silicone oil is often used to between heat sink and semiconductor devices. The surface flatness and roughness are important parameters in press-pack devices and heat sinks. If a surface is not flat, it will be exposed to an uneven mounting pressure, which can damage components. Press-pack devices are often designed with strict constraints in flatness and roughness. Ideally, the TIM would leave a direct metal-to-metal connection where possible, and perfectly fill any remaining gaps. In practical thermal design, the TIM layer carries thee most uncertainties. This comes from both irregularities and an the ageing phenomena. Semiconductor device manufacturers often specify an expected case to heat sink thermal resistance in data sheets.

3.5.3 Thermal Equivalent Circuit Models

Thermal analysis of devices is a complex problem, with many different mechanisms and parameters. A detailed model can be made using Finite Element Method (FEM), which can take into account temperature dependant parameters, as well as being able to show internal variations in the material.

More commonly, thermal analysis is done through an equivalent circuit model. These employ a thermal impedance network with parameters corresponding to those found in electrical circuit theory. The equivalent parameters are shown in **Tab. 3.4**.

Electrical parameters	**Thermal parameters**
Voltage U, $[V]$	Temperature difference, ΔT $[°C]$
Current I, $[A]$	Heat flow, Q $[W]$
Resistance, R $[\Omega]$	Thermal resistance, R_{th} $[°C/W]$
Capacitance, C $[F]$	Thermal capacitance, C_{th} $[J/°C]$

Table 3.4: Corresponding parameters between thermal and electrical networks

A thermal equivalent network translates a complex time response into a one dimensional model, where heat flows through the system and generates temperature differences within the system. Note that these kind of models are simplifications of the actual physical phenomena, such as the temperatures being treated as uniform. Thus, there are some limitations to the application of such models. However, they are widely employed in practical design.

Cauer Thermal Model

One of the thermal equivalent circuit models is the Cauer model. This representation ties directly to the physical properties of the device, as presented in the previous section. Because of this, it has a more intuitive connection to the real device. It requires considerable knowledge of the geometries and materials in the full device, in order to accurately describe the thermal behaviour. A general Cauer model is presented in **Fig. 3.13**

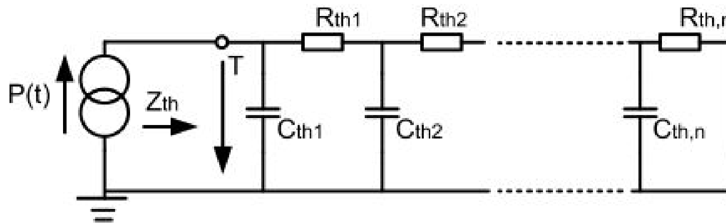

Figure 3.13: Cauer thermal equivalent model for heat transfer [108]

In this model, each RC-pair represents a layer in the path of heat flow from junction to ambient. One RC-pair for the silicon base, one for thermal grease, and so on. To improve accuracy, a layer can be divided into several RC-pairs.

Foster Thermal Model

A more empirical approach is found in the Foster model. The RC-pairs here do not have any direct physical meaning, but are merely representations of an analytical function. As such, it is a kind of ”black-box” model for thermal behaviour. A general Foster model is presented in **Fig. 3.13**

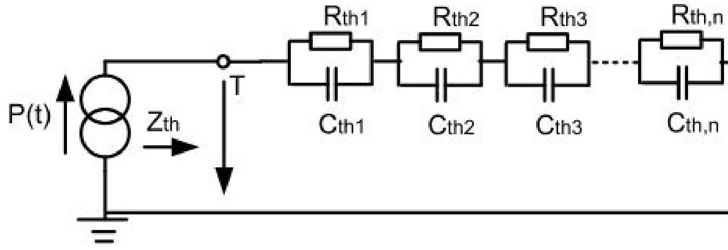

Figure 3.14: Foster thermal equivalent model for heat transfer [108]

The analytical function describing the thermal impedance of a device is given by equations (3.11) and (3.12).

$$Z_{th} = \sum_{i=1}^{n} R_{th,i}(1 - e^{\frac{t}{\tau_i}}) \tag{3.11}$$

$$\tau_i = R_{th,i}C_{th,i} \tag{3.12}$$

In practical cases, the foster model is the most widely used for thermal design. One reason for this is the IEC standard 60747-9 6.3.13, which provides strict guidelines for testing and measuring thermal impedance values. This gives a reliable standardization between different manufacturers. Therefore, data sheets usually provide values for a Foster analytical function.

3.5.4 Cooling System

The purpose of a cooling system is to ensure that the semiconductor devices stay within a reasonable operating temperature. The choice of operating temperature can vary depending on the device, application, or safety. However, the cooling system will always have to reliably control the temperature.

There are several different types of thermal management systems. The most common of these can be divided into natural or forced air cooling, liquid cooling, and phase change systems. There are some more advanced cooling systems proposed in research, but this paper will focus on the readily available and reliable technologies.

Natural Convection Cooling System

In terms of simplicity, a natural convection system is a good choice where applicable. The principle of operation is based on static extrusions allowing air to flow naturally around fins or pins. This is a very common solution for low power applications, where the cooling requirements are relatively low.

These heat sinks have the advantage of not requiring any applied force to function, meaning no external components are needed. They are simple, cheap and reliable. However, as stated earlier in the chapter, there is a substantial difference in heat transfer capability between natural and forced convection solutions. For high power devices, natural convection systems are often insufficient, and can not be used.

Specifically for press-pack stacks, natural convection heat sinks would require a solid and stable design, as it would need to withstand a high clamping force over a long time. Ideally, the effective area of the heat sink should be maximized, in order to get the best performance. This can be an issue with heat sink design, as mechanically weak constructions often give the best heat transfer performance.

Forced Air Cooling Systems

Forced air cooling uses the same philosophy as natural convection solutions. However, the convection effect is amplified by fans forcing air flow along the heat sinks. This means that a better heat transfer can be achieved while still maintaining a mechanically robust construction. Compared to liquid cooling, forced air cooling has the benefit of being simpler, and having lower power requirements. Only the fans need to be supplied auxiliary power, and the required work to pump air in an open system is much lower than for pumping liquids in a closed one.

The two most important parameters in a forced air cooling system are the volumetric flow of the air, and the heat spread through the heat sink fins. The flow rate can be increased by altering the geometry of the heat sink, or by increasing the fan power. The geometry of a heat sink dictates the pressure drop of the air flow, which correlates to the required fan power. To achieve a better base spreading, different materials can be utilized. A 2012 study [109] found that a force air cooled heat sink design could attribute close to 30% of its thermal resistance, from junction to ambient, to poor heat spreading in the base. The heat sink base spreading resistance was reduced from $12°C/kW$ to $5°C/kW$ by using a copper base in stead of aluminum.

In [81], a 1 MW bi-directional DC circuit breaker was designed, with two RB-IGCTs and forced air cooling. The design is shown in **Fig. 3.15**.

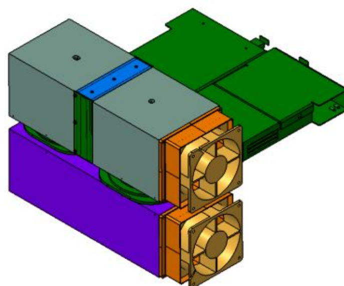

Figure 3.15: Forced air cooling system for two IGCT modules [81]

This design takes advantage of double-sided cooling possibilities of press-pack devices, and can achieve a much higher cooling performance compared to designs relying on

natural convection. If more devices need to be connected, however, each heat sink would be heated from both sides, and would be required to need to transfer more heat away from the power electronic devices.

There are some important drawbacks to forced air cooling. The ambient temperature is of high importance, meaning that a sufficient supply of air at low temperature is needed. During normal operation, the air around the circuit breaker would heat up to some extent, and may reduce the cooling capabilities of the system. This is especially true if space is limited, as the air inside a compartment would heat up to a higher temperature.

Liquid Cooling Systems

Liquid cooling systems have the advantage of of high heat transfer capabilities, due to the higher heat capacity of liquids. They are also less constricted in terms of space around the circuit breaker, as they can transfer the liquid and dissipate heat elsewhere. They are also more mechanically robust for use in press-pack stacks, and can be specifically designed in order to fit the device surface. However, the pumps required to drive a liquid cooling system add a layer of complexity, and require auxiliary power to run. An example of liquid cooled heat sinks is shown in **Fig. 3.16**.

Figure 3.16: Example of liquid cooled heat sink for press-pack IGCTs [110]

Liquid cooling utilizes a so-called "cold-plate" as contact surface, with a liquid flowing through and actively cooling the component. The choice of liquid has a significant impact on the system. Water is considered a good choice, due to its specific heat capacity at normal operating temperatures and its relatively low viscosity. This correlates to good heat transfer capabilities and low pump power requirements. When working in temperatures below $0°C$, a mixture of water and glycol is required to avoid freezing inside the system. This will not have a significant impact on the fluids viscosity, but the heat capacity will be lower, depending on the mixing ratio.

A basic liquid cooling system consists of a cold plate, a pump, a secondary heat exchanger towards the ambient, and tubing between these. For better performance, the secondary heat exchanger can be more efficiently cooled with a connected fan. The tubing should be based on a stiff material because of the thermal expansion and contraction forces.

Lastly, the heat sinks serve as electrical connections between the terminals. Thus, the water will have to be de-ionised and filtered, in order to keep conductivity low.

When designing a liquid cooling system, there are several parameters that can be altered for performance increase. One important design choice is how the liquid flows within the heat sink. A uniform internal temperature distribution is advantageous, which means a traditional heat exchange layout might be unsuitable. Additionally, the pressure drop through the heat sink should be kept low, in order to avoid slowing down the flow. **Fig. 3.17** shows two examples of internal tube layouts, considered in a paper concerning heat sink design for IGCTs. In this paper, the traditional S-type tubing was found to have an uneven surface temperature, and a high pressure drop, compared to the more complex Archimedes spiral layout [111].

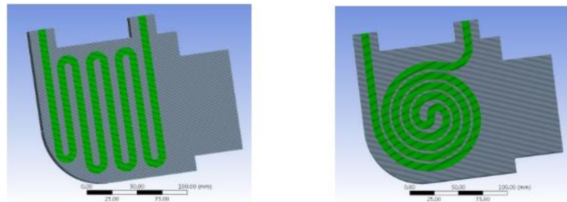

Figure 3.17: Left: S-type fluid tube. Right: Archimedes spiral fluid tube [111]

Another important parameter is the volumetric flow rate of the liquid. As for forced air cooling systems, the flow rate has a high impact on heat transfer performance, and can be designed to keep the temperature within reasonable bounds. Note that an increased flow translates to higher pumping power requirements, and the system still needs to effectively dissipate heat into the ambient.

Summary of Cooling Systems

A fully functional cooling system needs to be properly designed according to some key factors. These are listed below:

- **Required cooling power:** The necessary heat transfer, bounded by the defined maximum temperature of the device.
- **Liquid or air flow path:** The coolant path through the heat sink can have a dramatic impact on heat transfer capability. The whole device surface must be cooled, and blind spots must be avoided.
- **Pressure drop:** This is a defining factor for required power and volume of the fan or pump. A high pressure causes a poorer cooling performance for the same pump or fan capacity.
- **Thermal uniformity:** It is important to keep the temperature as stable as possible. This is because an optimized design has a good heat spread through the sink, and because a poor uniformity would lead to hot spots and potential local damage.

- **Material and mechanical requirements:** Some restrictions may be put on the cooling systems in terms of material usage and robustness. Press-pack systems need mechanical stability over time, and should avoid corrosion. Nickle or silver plating is commonly used in press-pack mounts.
- **Cost:** More advanced cooling systems are often more costly, both in terms of initial investment and maintenance. This should be minimized as far as it is possible.
- **Weight and size:** Depending on application, weight and size may be important constraints. Especially for transport applications, this is an important design goal.

The different types of cooling systems all have their applications, where some advantages may outweigh challenges. A summary of how the types relate to each other is shown in **Tab. 3.5**.

	Natural Convection	**Forced Air**	**Liquid Cooling**
Heat Transfer Capacity	Low	High	Very high
Cost	Low	Medium	High
Complexity	Very low	Medium	High
Power Requirements	None	Low	High
Compactness	Medium	Low	High
Controllability	None	Medium	High
Maintenance	Low	Medium	High

Table 3.5: Comparison of cooling systems

Note that compactness in this case refers to the specific mounts. Liquid cooled systems are heavier and require more available space, but are more flexible in terms of placement the secondary heat exchanger. Air cooled systems are dependant on some spacial clearing to achieve a good performance, and are more susceptible to local heating around the circuit breaker.

Chapter 4

Design of Solid-State Circuit Breaker

The design of a solid-state circuit breaker is a complex challenge, where a wide spectrum of components parameters can be altered and optimized for a better performing final design. For the purpose of thermal design, some assumptions will be made to focus on the thermal performance of the designs. A detailed transient model of the electrical performance during fault clearance is beyond the scope of the thesis, and will be limited to a brief analysis of passive component requirements.

This chapter will present designs for different power electronic devices. First, the system for which the circuit breaker is designed will be defined. Second, the relevant design considerations will be identified. Last, the different designs for circuit breakers will be analysed according to the specified design goals.

4.1 Design System

Simulations are carried out in Matlab and Simulink. The complete system is split into two models, one for electrical simulations, and one for thermal simulations. Note that any measurement components in the model are omitted in this chapter, for the sake of simplicity.

4.1.1 Electrical Model

The circuit diagram of the studied MVDC grid is shown in **Fig. 4.1**. Power is supplied by a DC voltage source, V_{DC}, S is the power electronic switching device. L_s, D_s, R_s and C_s are, respectively: Current limiting inductor, snubber diode, snubber resistor and snubber capacitor. R_1, R_2, L_1 and L_2 are the cable resistance and inductance between circuit breaker and load.

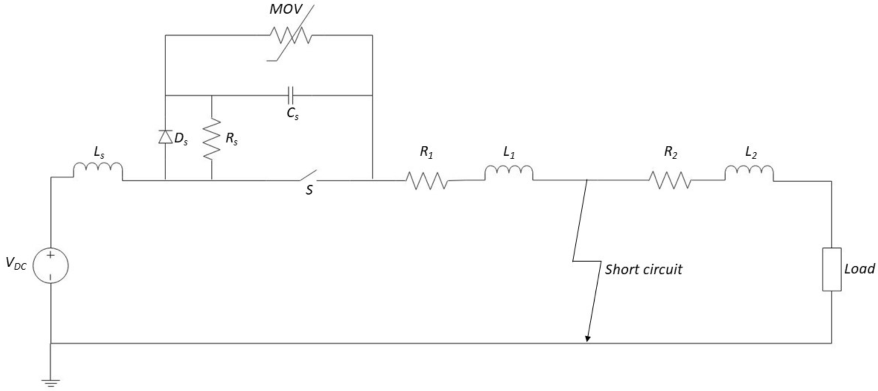

Figure 4.1: Circuit diagram of the MVDC grid

A summary of system parameters is given in **Tab. 4.1**. Note that the circuit breaker is designed to handle the worst case scenario, in which the fault occurs close to the source.

Parameter	Value
$V_{DC}\ [kV]$	3
$I_n\ [kA]$	1
$R_1\ [m\Omega]$	1
$R_2\ [m\Omega]$	1
$L_1\ [mH]$	0.1
$L_2\ [mH]$	0.1

Table 4.1: System parameters for the analysed MVDC grid

Faulted MVDC Grid

The Simulink model used for the electrical analysis is shown in **Fig. 4.2**. Power is supplied by a DC voltage source, which is protected by a circuit breaker. Two series RL-branches simulate the cable resistance and inductance between the circuit breaker and load. After a certain time, a zero-impedance fault occurs at the midpoint between circuit breaker and load.

Current Interrupting Solid-State Circuit Breaker

The block used to represent the circuit breaker is shown in **Fig. 4.3**. Current flows in through the CB in terminal , through the current limiting inductor L_s. During normal

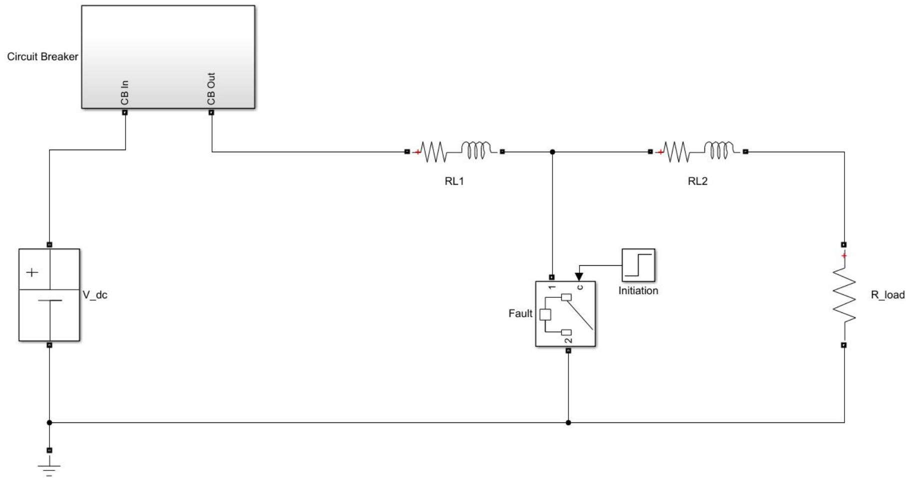

Figure 4.2: Simulink model of the MVDC grid, for electrical analysis

operation, current flows through the semiconductor device branch and out through CB out. When a gate signal turns off the device, the RCD-snubber and MOV are activated. Note that the MOV is modelled as an ideal diode. This will be explained in a later section. The turn-off of the device is instantaneous, whereas in a real situation, the transients presented in chapter 3.4 would occur. However this is sufficient for the purpose of the model.

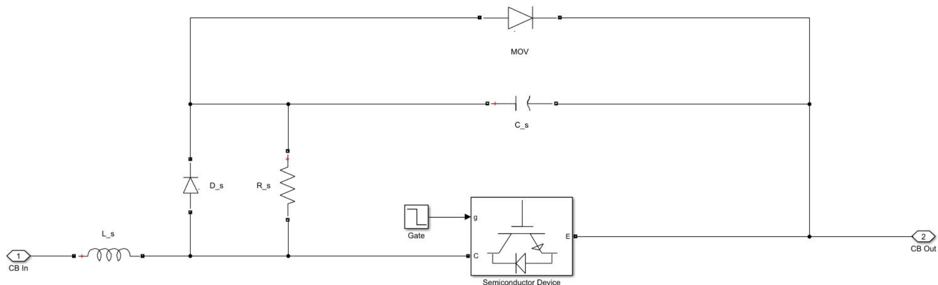

Figure 4.3: Circuit breaker block used in **Fig. 4.3**

4.1.2 Thermal Model

The thermal model for the power electronic device and cooling system is shown in **Fig. 4.4**.

The thermal resistance of devices, between junction and case, are given in data sheets by a set of four resistances and time constants. These are represented by R_1, R_2, R_3 and R_4, and the connected thermal capacitances. Thermal capacitances are calculated

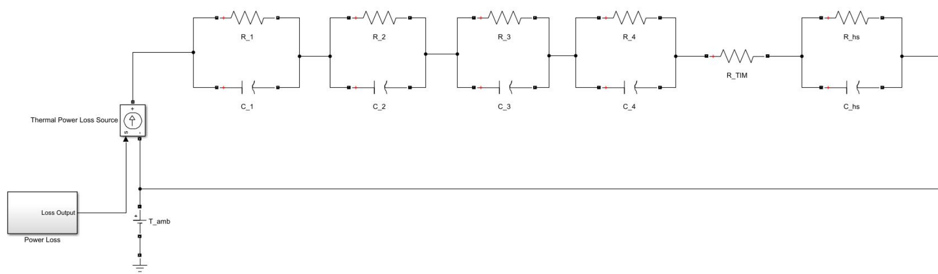

Figure 4.4: Simulink model for thermal analysis of the circuit breaker

through equation (3.12). R_{TIM} is a representation of the thermal resistance of the interface between case and heat sink. Expected values are usually given in data sheets, but is highly dependent on roughness and flatness of surfaces, as well as thermal grease and whether or not the device is properly cleaned prior to mounting.

$R_{th,hs}$ is the thermal resistance of the heat sink, and $C_{th,hs}$ is the thermal capacitance. These are free variables in a cooling system design. The purpose of the simulations are see the effects on $R_{th,hs}$ on the system, to pinpoint its required value for different cases, and to see the effects of various scenarios at fixed valued of $R_{th,hs}$. The thermal capacitance of the heat sink is not of any importance for this investigation. Typical values of heat sink time constants range from 4 minutes to 15 minutes [112]. These can be expected to be slightly lower for force cooled solutions, but the speed of breaking is too high for it to have any impact on the cooling performance. In order to avoid long simulation times, $\tau_{th,hs}$ is set to 4 seconds.

$T_{vj,max}$ and T_{amb} are, respectively, the maximum allowable temperature at the semiconductor junction and the ambient temperature. T_{amb} is dependant on location, as well as daily and seasonal variations. For the purpose of the analysis, ambient temperature is considered as relatively high, at $T_{amb} = 300K = 26.85°C$. $T_{vj,max}$ is an important constraint for semiconductors. At elevated temperatures, there is an increasing leakage current through the device, which in time degrades the junction, and may eventually lead to failure. A rule of thumb states that the rate of component failure doubles for every $10 - 15\%$ above $50°C$. For this analysis, the maximum temperature is set as $T_{vj,max} = 80°C$.

4.2 Design Considerations and Goals

The design goals provide a baseline for the process. The general criteria were briefly mentioned in chapter 3.3. They are revisited here:

- Low on-state losses
- Reliability
- Low ratings and number of semiconductor devices
- Minimizing passive components

- Low peak fault current
- Low breaking times

These conditions are often interconnected. In terms of cost, lower rated power electronic devices are often cheaper, but they also have higher on-state losses, and require bigger snubber circuits for same system ratings. It then becomes a matter of optimization and trade-offs.

To reiterate, the primary focus of this thesis is thermal performance, efficiency during conduction and reliability. A basic design in terms of requirements for passive components will be made, in order to give an idea as to the requirements of different designs. A full transient analysis, however, is beyond the scope of this paper.

4.3 Passive Component Design

This section will briefly discuss the design of passive components for a circuit breaker. The components in question are current limiting inductor, snubber capacitor, snubber resistance, and MOV. The design process will not consider any series or parallel connections, but some implications will be made clear where it is relevant.

4.3.1 Current Limiting Inductor

The purpose of a current limiting inductor is to protect the semiconductor device from excessive peak current or current rise. High inductor values protects the device from current stresses, but also increase the amount of magnetic energy that must be dissipated after turn-off. A high inductance value thus increases breaking times and turn-off losses.

In case of parallel connections, inductors may be utilized for transient current sharing between the different branches.

When designing a current limiting inductor, there are two restrictions that need to be considered, I_{max} and di/dt_{max}. I_{max} is the maximum current rating of the device, or specifically the maximum current at which the device is capable of turning off. di/dt_{max} is the maximum allowable current rise through the device.

In the worst case scenario, a zero-impedance fault occurs infinitesimally close to the circuit breaker, meaning that there is no impedance between circuit breaker and ground. The full nominal voltage V_{DC} is taken over by the circuit breaker, leading to a current rise as shown in equation (4.1).

$$V_{DC} = L_s \frac{di}{dt} \tag{4.1}$$

From this equation, we see that there will be a linear current rise from I_n after a fault occurs. The equation can then be linearized as in equation (4.2).

$$V_{DC} = L_s \frac{I(t) - I_n}{t} \tag{4.2}$$

For a specific device, there will be a turn-off time t_b, defined as in (4.3). Here, $t_{sensing}$ is the time delay from sensing and coordination, and t_{off} is the time it takes for the switch to turn off when the turn-off gate signal is received.

$$t_b = t_{sensing} + t_{off} \tag{4.3}$$

An inductance must be able to keep the current below maximum turn-off capability, the condition presented in equation (4.4)

$$V_{DC} = L_s \frac{I_{max} - I_n}{t_b} \tag{4.4}$$

From this discussion, we can derive the minimal inductance value is the maximum of equation (4.5) and (4.6).

$$L_{s,min} = \frac{V_{DC}}{\frac{di}{dt_{max}}} \tag{4.5}$$

$$L_{s,min} = \frac{V_{DC}}{\frac{I_{max}-I_n}{t_b}} \tag{4.6}$$

For IGCT devices, high rate of rise in current can be critical, because of the device topology. Being split up into different segments, a high rate of rise could lead to poor current sharing between the cathode segments. This could lead to local overheating, and so data sheets normally provide a di/dt_{max}. As a more homogeneous device, IGBTs are not limited in the same way, and so do not provide a di/dt_{max} in data sheets.

4.3.2 Snubber Capacitor

The snubber capacitor define the rate of voltage rise when the device turns off. They do not have any impact on maximum voltage over the device, as that is controlled by the MOV. The reason that a snubber is required for some devices is the overlap during turn-off, where the switch is still conducting, but the voltage starts to rise. This creates an increase in power dissipation, which might exceed the devices limitations.

In case of series connected switches, capacitors can also improve transient voltage sharing.

When designing a circuit breaker, maximum power dissipation P_{max} constricts the minimum value of snubber capacitance C_s. The connection is made through a series of steps, starting with the equation (4.7) defining power dissipation in the switch, P_S.

$$P_S(t) = v_S(t) \cdot i_S(t) = v_c(t) \cdot i_S(t) \tag{4.7}$$

The current through the switch is assumed to linearly fall to zero during the time interval between t_b and $t_b + t_f$. Here, t_f refers to the falling time of the current through the switch during turn-off. From this, the current through the switch becomes as shown in equation (**??**)

$$i_S(t) = I(t_b) - \frac{t}{t_f} I(t_b) \tag{4.8}$$

$v_c(t)$ is the instantaneous voltage across the capacitor, and is derived using equations (4.9) and (4.10).

$$i_c(t) = I(t_b) - i_S(t) = I(t_b) - (I(t_b) - \frac{t}{t_f} I(t_b)) = \frac{t}{t_f} I(t_b) \tag{4.9}$$

$$v_c(t) = \frac{1}{C} \int_{t_b}^{t} i_c(t) dt = \frac{I(t_b) t^2}{2Ct_f} \tag{4.10}$$

Combining these equations, we get the formula for turn-off heat loss through the device, as in equation (4.11). This has a maximum at $t = \frac{2}{3} t_f$, which leads to a maximum power dissipation as shown in (4.12). In the end, this gives the minimal requirement for snubber capacitor, as shown in (4.13).

$$P_S(t) = \frac{I(t_b)^2 t^2}{2Ct_f} (t^2 - \frac{t^3}{t_f}) \tag{4.11}$$

$$P_{max} = \frac{2I(t_b)^2 t_f}{27C} \tag{4.12}$$

$$C_{s,min} = \frac{2I(t_b)^2 t_f}{27P_{max}} \tag{4.13}$$

For IGCT devices, the power capability is normally sufficiently high that the turn-off operation does not exceed the maximum power requirements. In order to verify this, one can use the limiting load integral is given in data sheets.

4.3.3 Snubber Resistance

The purpose of a snubber resistor is primarily to reduce transient stresses on the switch, caused by resonant operation of the inductance and capacitance of the breaker.

In series connected switches, the resistor can also serve the purpose of static voltage sharing.

The function of a snubber resistor is a long discussion, which will not be held in this paper. Most importantly, the resistance should be high enough to avoid the system is not underdamped in its transient response after the MOV is deactivated. This requires the snubber resistance to be sufficiently high to keep the response critically damped or overdamped for all fault locations, and will therefore be designed for a worst case scenario where the fault occurs at the load. This provides the minimum snubber resistance from equation (4.14)

$$R_{s,min} = 2\sqrt{\frac{L_{tot}}{C_s}} = 2\sqrt{\frac{L_s + L_1 + L_2}{C_s}} \tag{4.14}$$

Note that the snubber setup is not ideal in terms of the snubber diode. A high snubber resistance leads to high voltage stress on the diode, which means the snubber diode must have a higher voltage rating to avoid breakdown. In more realistic cases, a trade-off must be made between R_s and D_s.

4.3.4 Metal-Oxide Varistor

The MOV in a current interrupting solid-state circuit breaker has two functions. First, they clamp the voltage across the semiconductor switch to a set value. Secondly, they dissipate any residual magnetic energy in the system. The two most important characteristics of a MOV for circuit breakers are the clamping voltage, V_{cl}, and resistance, R_{MOV}. In addition, there will be some leakage current flowing through the MOV during normal conduction, causing some conduction losses.

When the circuit breaker is triggered, the maximum voltage across the solid-state switch will be dictated by the MOV. The maximum clamping voltage is thus given by equation (4.15), with a lower constraint given by equation (4.16). A higher clamping voltage will increase the breaking speed, but will also increase the maximum voltage across the semiconductor switch, and he peak fault current. R_{MOV} should be minimized for improved performance.

$$V_{cl}^{max} = V_{max} - R_{MOV} I_{f,max} \tag{4.15}$$

$$V_{cl}^{min} = V_{DC} + R_{MOV} I_{f,max} \tag{4.16}$$

The use of MOV is an important topic in itself. However, the proper design of one is omitted in this paper. The MOV in the simulations is modeled as an ideal diode with a forward voltage at 110% of V_{DC}.

4.4 Properties of the Circuit Breakers Designs

From the discussion in the previous chapter, a current interrupting solid-state circuit breaker was found to be thee best choice for fault handling in MVDC systems. As the greatest challenges of this topology are related to current stresses, on-state losses and thermal management, the choice of power electronic devices for the breaker will be crucial.

The most promising devices were found to be the IGBT, the IGCT and the BIGT. Five different devices are investigated; two IGCT, two IGBT and one BIGT. The properties of the chosen devices are shown in **Tab. 4.2**. The IGCTs and IGBTs are separated into one with high current rating, and one with low current rating. The devices rated for lower current are expected to have poorer performance, but the cost benefit may be considerable when designing a full scale grid with several circuit breakers. The high-current-capability IGCT, 5SHY 35L4522, is denoted as $IGCT_1$. The high-current-capability IGBT, 5SNA 2000K450300, is denoted as $IGBT_1$. The low-current-capability IGCT, 5SHX 26L4520, is denoted as $IGCT_2$. The low-current-capability IGBT, 5SNA 1300K450300, is denoted as $IGBT_2$. The BIGT, 5SJA 3000L520300, is denoted as $BIGT$

Device	$IGCT_1$	$IGBT_1$	$IGCT_2$	$IGBT_2$	$BIGT$
V_{max} $[kV]$	4.5	4.5	4.5	4.5	5.2
I_{max} $[kA]$	4	4	2.2	2.6	6
V_{on} $[V]$ $(1kA, 125°C)$	1.32	2.44	2.23	3.02	2.23
$R_{th,j-s}$ $[°C/kW]$	11.50	5.05	16.80	7.58	3.05
di/dt $limit$ $[A/\mu s]$	1000	High	100	High	High
$P_{max}[kW]$	High	25	High	16.7	55.5
LxWxH $[mm]$	439x173 x41	246.95x237.3 x28.75	439x173 x41	246.95x237.3 x28.75	237x250 x31.5

Table 4.2: Characteristics of the different power electronic devices (From data sheets)

These values are used in simulations and in order to calculate the required passive components.

Chapter 5

Simulations, Results and Discussion

The purpose of the different scenarios is to investigate how the performance of the devices vary with different conditions. This is done in order to compare the performance at different operating conditions, as well as to evaluate the sensitivity of various parameters.

Note that all results reflect the steady state condition. This choice was made because the impact of breaking operation is minimal, in terms of thermal performance and total losses. In terms of the electrical stresses, the designed to handle the worst case scenario, and should operate reliably. In the thermal model, thanks to the thermal time constants and the fast turn-off process, the added stress from breaking operation is negligible.

Case 1 and 2 will be used to compare the different devices under varying conditions. Case 1 looks at devices under different nominal current, both singular devices and two parallel connected devices. In case 2, the power rating is kept constant, while nominal voltage and current is altered. The foregoing analysis will be used to make a choice of the most promising device for use in a solid-state MVDC circuit breaker. This device will used in the later case simulations. In cases 3, 4 and 5, a sensitivity analysis will be performed. Case 3 shows the effect of varying the thermal resistance between case and ambient. Case 4 looks at the effects of varying ambient temperature. In case 5, the effects of changing junction temperature restrictions are investigated.

The chapter is laid out as follows: First, the findings of the basic scenario is given. Next, the comparative study of cases 1 and 2 will be presented, showing the performance of different devices. Next, the results from sensitivity analysis of cases 3, 4 and 5, will be shown and interpreted. Last, some additional remarks will be made to clarify some factors and issues.

5.1 Base Case Scenario

The base case scenario for the simulation is the primary design scenario for the circuit breaker. The system operates as a $3MW$ grid at $V_{DC} = 3kV$ and $I_n = 1kA$. At these ratings, all studied devices will be able to operate without series or parallel connections. $T_{vj,max}$ is set at $80°C$, and T_{amb} is assumed to be $300K$.

The devices will be compared in their cooling requirements and losses at steady state temperature, based on the maximum allowable $R_{th,hs}$ and conduction losses P_{on}. The worst performing device will then be used as a baseline for comparing the devices in terms of their steady-state virtual junction temperature T_{vj} at a fixed thermal heat sink resistance. Additionally, the passive component requirements to ensure stable and reliable breaking, will be shown. Finally, the time it takes for the fault current to be brought to zero is given, to evaluate whether there are any significant differences.

Results

The results of the base case calculations and simulations are shown in **Tab. 5.1**. In the table, P_{on} is the conduction losses of the device, $R^{max}_{th,hs}$ is the maximum allowable thermal resistance of the cooling system, T_{vj} is the virtual junction temperature at a fixed $R_{th,hs}$, and L_s, C_s and R_s are the passive component requirements. t_{clear} is the time it takes for the fault to be fully cleared.

Device	$IGCT_1$	$IGBT_1$	$IGCT_2$	$IGBT_2$	$BIGT$
P_{on} $[W]$	1324	2441	2233	3019	1963
$R^{max}_{th,hs}$ $[°C/kW]$	28.65	16.72	7.01	10.03	20.76
T_{vj} $[°C]$	51.35	56.25	80.00	70.95	46.65
L_s $[\mu H]$	16.00	10.00	30.00	16.31	4.82
C_s $[\mu F]$	-	11.85	-	15.08	6.54
R_s $[\Omega]$	-	6.09	-	5.55	8.01
t_{clear} $[ms]$	0.56	0.6	0.56	0.65	0.51

Table 5.1: Results of the base case scenario simulations

The results in **Tab. 5.1** show that the $IGCT_1$ has substantially lower losses than the other devices. The second best is the $BIGT$. The results are to be expected, due to the IGCT being a thyristor-based device. IGBTs have higher conduction losses, but the BIGT structure improves this to some extent through the increased area available for conduction.

The cooling system requirements are also lowest for the $IGCT_1$, although the difference is slightly lower than for the losses. When a fixed thermal resistance was used, the $BIGT$ showed the lowest T_{vj}, with the $IGBT_1$ and $IGCT_1$ devices being relatively close. This is due to the superior heat transfer capability of the IGBT structure, compared to the IGCT.

The current limiting inductor requirements are relatively high for IGCT devices, as they have a longer turn-off delay. Here, the $BIGT$ has the lowest requirements, due to its fast switching and high current rating. As expected, the $IGCT_2$ and $IGBT_2$ devices

need a higher inductance to avoid high current stresses. For a single device, IGCTs do not require an RCD-snubber. However, this is not the case for series connected devices. Of the other devices, the $BIGT$, have the lowest snubber capacitor requirements, but also higher resistor requirements. As previously mentioned, the full design of passive components is a more complicated study, but the initial design is sufficient for comparison.

The fault clearance times are relatively similar, ranging from $0.51ms$ for the $BIGT$, to 0.65 for the $IGBT_2$.

5.2 Comparative Study

The results of the base case are a good starting point for further analysis. In this section, the devices are evaluated at a wider range of operating conditions.

5.2.1 Case 1: Varying Nominal System Current

In this case, the voltage will be kept constant, and the nominal system current will be varied between $500A$ and $2000A$ with one device. A secondary analysis will be done with 2 parallel connected devices, with nominal current between $1000A$ and $4000A$. The heat sink resistance will be kept constant.

The purpose of this case is to look at the performance of the different devices under varying current stresses. The comparison will be made based on junction temperature T_{vj} and conduction losses P_{on}.

Results

The simulation results are shown in **Fig. 5.1**, **Fig. 5.2**, **Fig. 5.3** and **Fig. 5.4**.

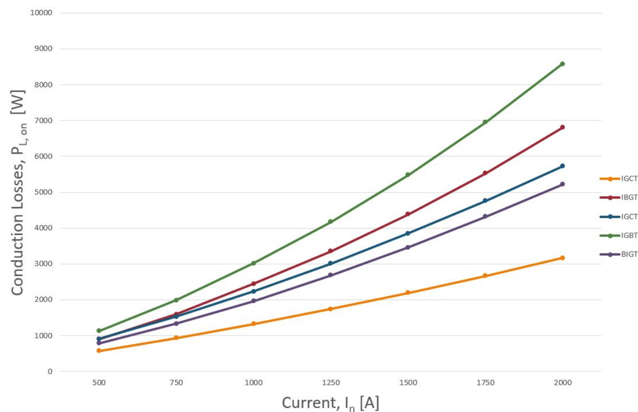

Figure 5.1: Conduction losses at varying current for a single device.

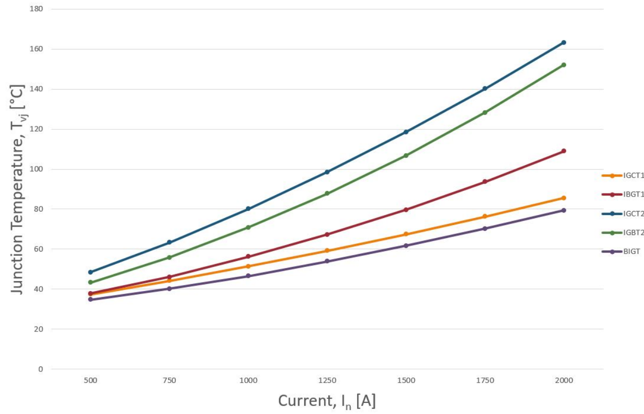

Figure 5.2: Junction temperature at varying current for a single device.

Fig. 5.1 shows the conduction losses of the singular devices, and **Fig. 5.2** shows the virtual junction temperature, at different nominal system current. Similarly to the base case, the $IGCT_1$ and $BIGT$ have the best performance overall. The graphs show that the advantage of the $IGCT_1$ becomes even more significant at higher current. Similarly, the junction temperature for the $BIGT$ and $IGCT_1$ is more stable at higher current than for the other devices.

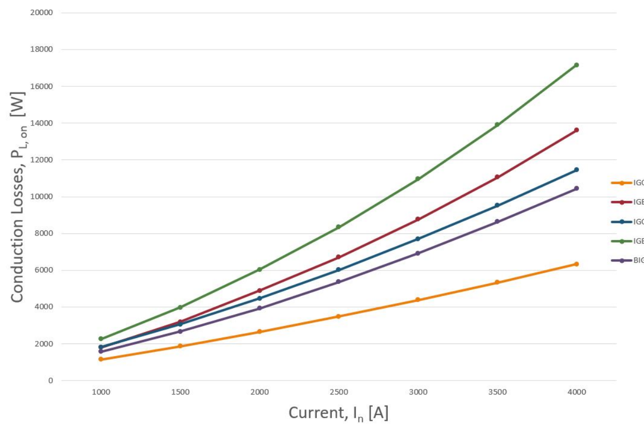

Figure 5.3: Conduction losses at varying current for two paralleled devices.

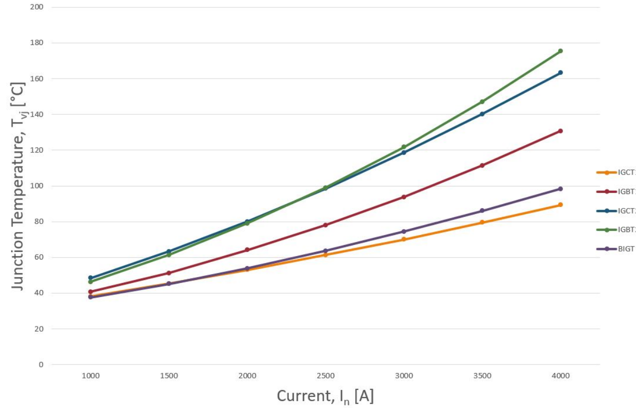

Figure 5.4: Junction temperature at varying current for two paralleled devices.

Fig. 5.3 shows the conduction losses and **Fig. 5.4** shows the virtual junction temperature, of two parallel connected devices at different nominal system current. In terms of losses, the mechanisms are similar to what was found for a single device. The thermal behaviour, however, has some notable changes. For one, the $IGCT_1$ outperforms the $BIGT$, as the conduction loss benefit of the IGCT outweighs the internal heat transfer capability of the BIGT.

5.2.2 Case 2: Varying Current and Voltage at Constant Power

In this case, the power rating of the grid will be kept constant, at $6MW$. The system voltage will be varied between $3kV$ and $9kV$. At higher voltages, more devices will need to be connected in series to achieve the rated blocking voltage. The heat sink resistance will be kept constant.

A comparison will be made based on junction temperature T_{vj} and conduction losses P_{on}. This will show how the devices perform for a constant power requirement, with varying current and voltage ratings.

Results

The simulation results are shown in **Fig. 5.5** and **Fig. 5.6**.

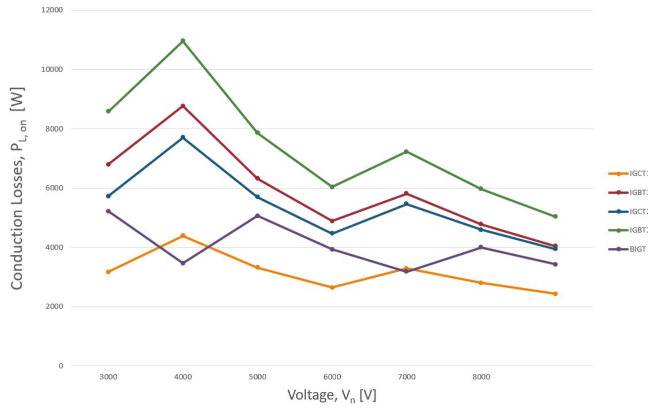

Figure 5.5: Conduction losses at varying nominal voltage, with constant power at $6MW$.

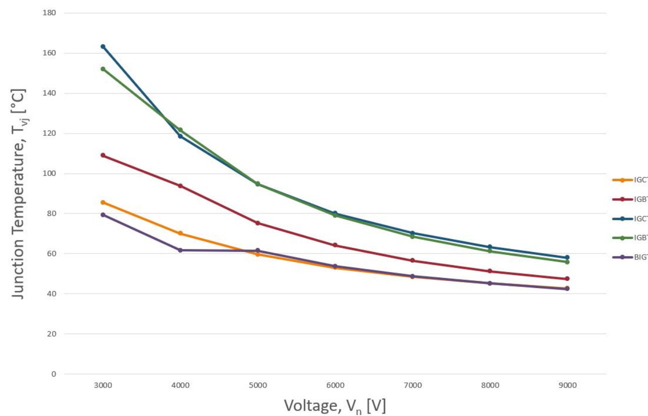

Figure 5.6: Junction temperature at varying nominal voltage, with constant power at $6MW$.

Fig. 5.5 shows the results of conduction losses for the different devices. For higher system voltages, the current is reduced, leading to lower conduction losses. When more devices are connected in series, the losses go up, as the full system current runs through an additional device. Except for the $BIGT$, which has a rated blocking voltage of $5.2kV$, all devices are rated at $4.5kV$. This can be seen by the jumps in the graph, where the $BIGT$ can achieve the lowest losses at some voltage levels. Apart from these voltage levels, the $IGCT_1$ has the lowest losses overall. Again, the IGBTs and $IGCT_2$ have the poorest performance.

In **Fig. 5.6**, the thermal performance at fixed heat sink resistance is shown. At lower voltages, the BIGT performs best. With increasing voltage, the gap closes in, with an almost indistinguishable difference in junction temperature from $BIGT$ to $IGCT_1$.

5.3 Selection of Power Electronic Device

From the results of the base case and comparison at various current and voltages, it seems clear that $IGCT_1$ is the best choice of semiconductor device for circuit breaker applications. Numerous studies on solid-state circuit breakers have pointed to conduction losses as the most critical developmental barrier. The superior conduction of the thyristor-based IGCT then becomes a major advantage compared to other devices. The $IGBT_1$ showed some beneficial traits in terms of thermal performance, but did not outperform the $IGCT_1$ in any of the studied cases. the $IGCT_2$ and $IGBT_2$ gave the poorest overall performance. In thermal performance there were no significant differences, but the conduction losses were much lower for the $IGCT_2$.

The only device that was able to compete with the $IGCT_1$ was the $BIGT$. The difference in performance was low for most situations. Under some conditions, the $BIGT$ even performed better than $IGCT_1$. The turn-off process of the $BIGT$ is also better than the other devices, leading to faster fault clearance and lower passive component requirements.

From the analysis, $BIGT$ might be beneficial in some cases. In general, however, the $IGCT_1$ will be the best choice, and will thus be selected for further analysis.

5.4 Sensitivity Analysis

5.4.1 Case 3: Varying Thermal Resistance

In this case, the electrical system parameters of the base case are kept. The base case thermal resistance requirement will be used as a starting point, and variations from $-6°C/kW$ to $+6°C/kW$ are applied. The junction steady state temperature T_{vj} and conduction losses P_{on} will be measured for each iteration.

The purpose of this case is to look at how the circuit breaker would react to changes in thermal resistance. This can be caused by a number of occurrences. The mounting could have been poorly done, a change in cooling fluid flow could happen, or the TIM may have degraded over time. For the purposes of the steady-state analysis, the changes will be applied to the thermal resistance of the heat sink. A change at the interface between device and cold plate would be analogous. As thermal resistance is a temperature-dependent parameter, this can show some implications of increase or decrease in thermal performance due to temperature fluctuations.

Results

The simulation results are shown in **Fig. 5.7**.

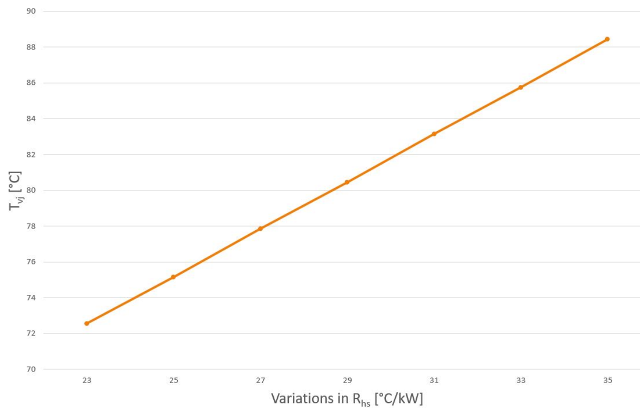

Figure 5.7: Junction temperature at varying thermal resistance.

From the graph, we can see a linear dependency on the thermal resistance. For every incremental change in thermal resistance, the junction temperature increases by approximately $1.35°C$. This indicates that, although not critical to the operation, it is worth to take note of. The cooling fluid flow can easily be designed to specification.

An observation can be made as to local changes in heat transfer capability. In case of poorly mounted stacks, or degraded thermal grease, hot spots can arise. These hot spots will have a higher rate of degrading, which may lead to an even higher local thermal resistance. Because of this, it is important to assure even temperature distribution. For reference, thermal interface resistance for press-pack devices typically range from 0.5 to $5°C/kW$. From this, one can assume that a certain variability may occur. Especially for poorly cleaned surfaces or uneven mounting, this can be critical. The temperature increase is not high enough that there is any immediate risk of component failure under these conditions. However, it is high enough that lifetime of the circuit breaker may be significantly reduced.

5.4.2 Case 4: Varying Ambient Temperature

In this case, the electrical system parameters of the base case are kept. The ambient temperature T_{amb} will be varied between $0°C$ and $60°C$. The junction steady state temperature T_{vj} and cooling requirements $R^{max}_{th,hs}$ will be measured for each iteration.

The purpose of this case is to look at the effects of different atmospheric conditions. Ambient temperature is a parameter that is susceptible to major fluctuations throughout the life cycle of a circuit breaker. Note that the ambient temperature refers to the available ambient for heat transfer. In an enclosed space, the effective ambient temperature may rise over time. The cooling system will be required to handle all possible states, and some specific limitations should be identified for a practical design.

The simulation results are shown in **Fig. 5.8** and **Fig. 5.9**.

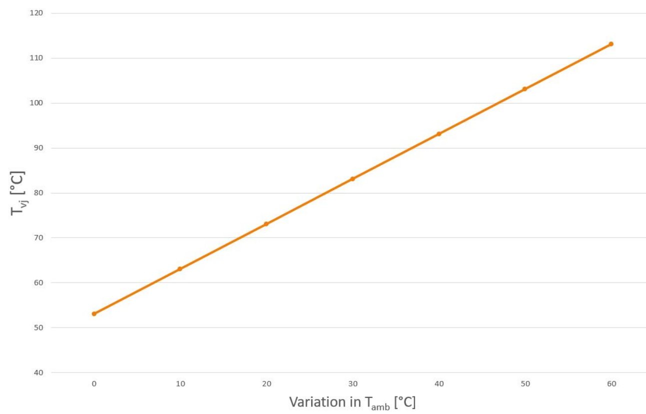

Figure 5.8: Junction temperature at varying ambient temperature.

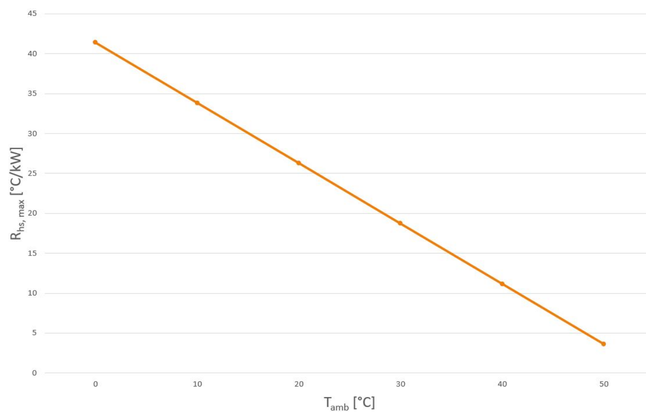

Figure 5.9: Maximum thermal heat sink resistance at varying ambient temperature.

Fig. 5.8 presents the virtual junction temperature of the device as a function of ambient temperature. This shows a close correlation between the two. The same can be said for cooling system requirements in order to keep temperature steady at $80°C$, as shown in **Fig. 5.9**.

The most important observation from these graphs is that there is a significant correlation between ambient temperature and thermal performance. In a practical design, the cooling system will be required to handle the maximum ambient temperature, and must be designed for this. Especially air cooled systems are susceptible to ambient temperature increase. In an enclosed space, the heat dissipated from the heat sink will linger, and there must be sufficient heat transfer towards the external environment.

An argument can be made from the results presented above, that there may be a considerable advantage to keep the circuit breaker within a controllable environment. If ambient temperature can be regulated to some extent, a significant gain can be made in terms of

the cooling system. This would add another degree of complexity to the system, but could also lower the ratings of the cooling system to some extent.

5.4.3 Case 5: Varying Maximum Temperature Restrictions

In this case, the electrical system parameters of the base case are kept. The maximum virtual junction temperature $T_{vj,max}$ will be varied between $60°C$ and $100°C$. The cooling system requirements $R_{th,hs}^{max}$ will be measured for each iteration.

The purpose of this case is to investigate the impact on constraining or relaxing the operating temperature requirements for the semiconductor device. This can have a significant impact on the reliability and performance of the devices, and an overview of the sensitivity to temperature restrictions is important.

Results

The simulation results are shown in **Fig. 5.7**.

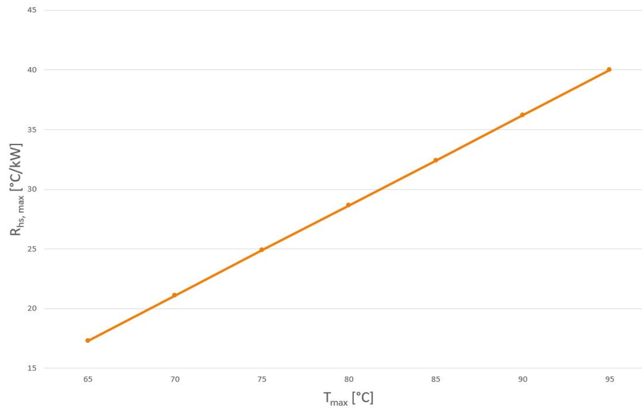

Figure 5.10: Maximum thermal heat sink resistance at varying temperature restrictions.

The graph shows a linear dependency of the junction temperature restrictions on the cooling system requirements. If the maximum junction temperature for the device is lowered, then the cooling system will also have to be scaled up to compensate. It should be noted that a small change in temperature restrictions has a substantial impact on cooling requirements. This means that a simpler and cheaper cooling system can be used, if the junction temperature is allowed to increased further.

As previously stated, the junction temperature has an impact on the reliability and performance of the circuit breaker. At higher temperatures, the risk for component failure is higher, and with a positive temperature coefficient the conduction losses will also increase. For a practical design, a trade-off must be made between the performance and reliability of the power electronic device, and scaling of the cooling system.

5.5 Thermal Performance of Cooling Systems

The main design criteria for the cooling system is the effective thermal resistance of the heat sink. This has also been the parameter for comparison in the simulations. In order to have an understanding of the practical implications, the associated values must be connected to commercially available. The lack of tailored cooling system designs for MVDC circuit breakers complicate the task of finding realistic values for heat sink resistance.

From literature, some values can be gathered. State of the art forced air cooling systems viable for IGCTs have been reported around $36.8 - 95.6°C/kW$ [81, 113, 114]. Scaled for IGBTs, heat sink resistance has been reported as low as $11.75 - 28°C/kW$ [113, 115]. High performing liquid cooling systems have been reported at around $1.7 - 14.3°C/kW$ [111, 113, 116, 117].

As stated earlier, there are several free variables when it comes to the design of cooling systems. The values provided here are only meant to give an overview of what can be expected from cooling systems. Comparing these to the studies made in this paper, it becomes clear that a liquid cooling system is the best choice. Such a system should be able to sufficiently dissipate the heat generated from a solid state MVDC circuit breaker, and also handle the varying conditions faced by said circuit breaker. The liquid cooled system should be able to handle varying conditions as shown in the sensitivity analysis, as long as it is properly designed. For forced air cooled systems, the ambient temperature is an especially sensitive parameter. A large volume of accessible air is required to dissipate heat. In a confined space, the low heat capacity of air could lead to locally increased temperatures around the circuit breaker. Looking at the reported heat sink performance, and comparing to **Fig. 5.9**, it becomes clear that a forced air cooled system may not be able to properly operate at elevated ambient temperatures.

In terms of applicability, there is some observations for different devices. The rectangular packaging and connectors make the force air cooled solutions more sensible for these devices. Additionally, the increased surface area available for thermal conduction to heat sinks are more substantial. The circular shape of IGCT connectors make forced air cooling systems more challenging, as a rectangular heat sink would compromise the heat spread through the sink base.

For a proper design, the performance requirements of a cooling system must be weighed up against cost and complexity. The analysis show that forced air cooling may be sufficient for some applications. This is especially true if the BIGT is chosen, as a bigger surface area is available for conduction. However, this may come at a cost of lower reliability and higher conduction losses. For each distinct application, a multi-variable optimization should be performed.

5.6 Additional Remarks

The simulations performed in this paper give a good overview of the thermal management of solid-state circuit breakers. There are however some aspects that are not covered in the analysis. This will be covered in this section.

5.6.1 Impact of Junction Temperature on Devices

In this report, the temperature dependence of various parameters has been neglected. To be within acceptable bounds, the design process has relied on a worst case approach, wherein parameters are gathered for a junction temperature of $125°C$. In a real application, temperature will be kept much lower. This can have a significant impact on temperature-dependent variables. These include failure rates which was covered earlier, conduction losses, and material heat transfer capabilities.

Depending on the device, temperature has a significant impact on conductive properties of a device [118]. This comes mainly from the charge mobility dependence on temperature. A positive temperature coefficient means that conduction capability is reduced at elevated temperatures.

The utilised models in this report do not handle any temperature-dependent thermal impedance. This is a significant defect when looking at the variability in parameters. Aluminum and copper are relatively stable materials, but silicon has a substantial temperature dependency. From $125°C$ to $75°C$, the thermal conductivity and heat capacity go from $98.9W/m°C$ and $788.3J/kg°C$ to $119W/m°C$ and $757.7J/kg°C$ [108].

5.6.2 Transient Thermal Response

As previously stated, the transient response to the breaker clearing a fault is omitted from the analysis, due to the fast operation. Note that this is due to a shortcoming of the equivalent circuit model. The temperature in device is represented as a virtual average junction temperature. Because of the fast response, the heat capacity of the material becomes even more important, as the heat generation propagates through the material. Hot spots and local silicon degradation may prove critical in a practical design.

5.6.3 Improved Analysis through FEM Simulations

As explained in this section, the thermal equivalent circuit models lack some important characteristics for an accurate analysis. For steady-state operation, these numbers serve as a good approximation. In order to fully understand the thermal behaviour of devices, a FEM model should be utilized. This has been established as a well-performing analysis tool, providing accurate and precise values.

For cooling system design, this should also rely on FEM simulations. In this paper, the performance of cooling systems has been simplified as an equivalent thermal resistance value. This is sufficient in terms of a comparable parameter, and a dimensioning baseline for a full design. In order to properly design a cooling system, however, FEM models are needed. For liquid cooled systems, this can be used to investigate the requirements of fluid flow, heat sink geometry, type of cooling fluid, and more. For cooling systems relying on air convection, the thermal spread through heat sink fins are important for the cooling performance, as well as air flow and movement across the fins.

Chapter 6

Conclusions and Further Work

6.1 Conclusions

This paper has gone through a number of steps in the design of a circuit breaker. Current literature on MVDC circuit breakers has been studied, and some conclusions have been drawn. Cooling requirements for some designs have been analysed for different cases. Some state of the art power electronic devices were compared to find the best choice for circuit breakers, with a primary focus on efficiency and thermal performance. The findings of the report are summarized in this section.

The first part was centered around the choice of topology of a MVDC circuit breaker. The mechanical and hybrid categories were found to be insufficient for handling the rapidly rising fault currents of a MVDC grid, whereas the solid-state circuit breaker was found to have some critical advantages. The biggest drawback comes from the conduction losses and heat management during on-state operation. The speed of operation, however is the most important aspect. This was also made clear in choice of topology between the different types of solid-state circuit breakers. The current interrupting breaker was the best performing in terms of fault clearance time, and is a simple and scaleable design. The current limiting, resistive and resonance topologies had their advantages, and will likely have their applications. For an overall analysis, however, the current interrupting solid-state circuit breaker has been found to be the best choice.

Five different power electronic devices have been investigated. A high-current-rated IGCT and IGBT, a low-current-rated IGCT and IGBT, and the newer BIGT device. These were compared according to their electrical performance, with respect to passive component requirements and conduction losses. For thermal performance, an initial thermal resistance requirement of the heat sink for each device was found. The virtual junction temperature with a fixed heat sink performance was then compared. This was done for both varying system current and parallel connections, and for varying DC voltage at fixed power and series connections. The high-current-rated IGCT was found to be the best performing device. The IGBT devices showed better thermal properties by themselves, but this effect was outweighed by the reduced heat generation from the IGCT. For this device,

the conduction losses were found to be $1.324kW$, and the maximum thermal heat sink resistance was found to be $28.651°C/kW$ The closest competitor was the BIGT. Due to its higher blocking voltage, the BIGT performed better at some voltage levels where other devices would require series connection. In the base case, the conduction losses of the BIGT were found to be $1.963kW$, and the maximum thermal heat sink was found to be $20.763°C/kW$.

With the high-current-rated IGCT chosen as the most promising device, a sensitivity study was performed, to analyse the impact on changing parameters. Variations in thermal resistance, either caused by poor thermal interface between device and heat sink, or change in cooling system performance, was found to have some impact on the junction temperature. This was not deemed to be critical to operation, but may cause further localized degrading and decreased lifetime of components. The ambient temperature was found to have a significant impact on cooling performance. An elevated ambient temperature may lead to the cooling system not being able to sufficiently dissipate heat from the circuit breaker, if not scaled for the right conditions. Here, a liquid cooled system has the benefit of dissipating heat in a separate environment, meaning a compact circuit breaker is achievable, as long as a sufficiently large space is accessible. The variations in maximum allowable junction temperature gave some insights, as a small change in temperature restrictions may be defining in a choice of cooling system.

The liquid cooling system was found to have several beneficial traits. The cooling performance is high enough to handle varying conditions, as long as the design is done properly. The mechanical stability and compactness are important for press-pack mounts, and especially for the chosen IGCT, which has a relatively low surface area available for conduction. The biggest drawbacks of a liquid cooling system are the cost, auxiliary power requirements and weight. Depending on the application, different traits may make forced air cooling more sensible.

6.2 Further Work

The MVDC circuit breaker is still in its early development phase. Power electronic devices are rapidly evolving, making the concept of a MVDC grid ever more feasible. Thermal management of power electronic devices in particular is still a subject that needs more research in the future. This paper serves as an initial overview of cooling requirements and the thermal performance of currently available devices and cooling systems.

Although the study of WBG devices was omitted from this report, these are expected to rapidly rise in voltage and current capability in the near future. As these devices have many beneficial traits, they should be considered for MVDC breakers as they reach a certain level of maturity. Additionally, more advanced cooling systems should be analysed in order to pinpoint possible developments in thermal management.

For a more thorough analysis of the power electronic device, a FEM model should be created. A more precise analysis should be made, which includes the variability in both electrical and thermal performance. The impact of different tripping times due to fault sensing and coordination, changes in current limiting inductance, as well as dynamics and stray components are important parameters of a detailed analysis. These are not properly covered in the simplified system model used in this paper. Thermal equivalent circuit

models are not sufficient to capture the complex thermal behaviour of a semiconductor device, especially the dynamics.

For the cooling systems, FEM models should also be made. Both forced air and liquid cooling should be designed, according to the constrains defined in this paper. Forced air cooled systems should be investigated thoroughly by varying different parameters, such as heat sink geometry, fan volume and power, as well as the external conditions used in this report. Liquid cooled systems should be investigated through a different set of parameters. Pumping power and volumetric liquid flow are important design points. The size and geometry of the heat sink itself are also crucial, and should be optimized for specific devices. Again, a more accurate sensitivity analysis can be made through FEM simulations. A precise evaluation of the performance of power electronic devices and heat sinks working together should be made.

In summary, the system models and findings of this paper should be connected to FEM models to gain an intricate understanding of the thermal management of a solid-state MVDC circuit breakers. This would provide the means to design and optimize cooling solutions for future applications.

Bibliography

[1] L. De Andrade and Teresa Ponce De Leao. A Brief History of Direct Current in Electrical Power Systems. In *2012 3rd IEEE HISTory of ELectro-technology CONference: The Origins of Electrotechnologies*, 2012.

[2] Michael Starke, Leon M. Tolbert, and Burak Ozpineci. AC vs. DC Distribution: A Loss Comparison. In *2008 IEEE/PES Transmission and Distribution Conference and Exposition*, 2008.

[3] Marene Larruskain, A J Mazon, and Oihane Abarrategui. Transmission and Distribution Networks: AC versus DC, 2014.

[4] Arne Hinz, Marco Stieneker, and Rik W. De Doncker. Impact and Opportunities of Medium-Voltage DC Grids in Urban Railway Systems. *2016 18th European Conference on Power Electronics and Applications, EPE 2016 ECCE Europe*, pages 1–10, 2016.

[5] Mehdi Monadi, M. Amin Zamani, Cosmin Koch-Ciobotaru, Jose Ignacio Candela, and Pedro Rodriguez. A Communication-Assisted Protection Scheme for Direct-Current Distribution Networks. *Energy*, 109:578–591, 2016.

[6] Gregory F Reed, Brandon M Grainger, Adam R Sparacino, Emmanuel J Taylor, Matthew J Korytowski, and Zhi-hong Mao. Medium Voltage DC Technology Developments , Applications , and Trends. *Cigre*, pages 1– 7, 2012.

[7] Marco Liserre, Roberto Cardenas, Marta Molinas, and Jos Rodriguez. Overview of Multi-MW Wind Turbines and Wind Parks. *IEEE Transactions on Industrial Electronics*, 58(4):1081–1095, 2011.

[8] H B G Casimir and J Ubbink. The Skin Effect. *Philips Technical Review*, 28(9):271–283, 1967.

[9] Jackson John Justo, Francis Mwasilu, Ju Lee, and Jin-Woo Jung. AC-Microgrids Versus DC-Microgrids with Distributed Energy Resources: A review. *Renewable and Sustainable Energy Reviews*, 24:387–405, 2013.

[10] L.A. Koshcheev. Environmental Characteristics of HVDC Overhead Transmission Lines. In *The Third Workshop on Power Grid Interconnection in Northeast Asia, Vladivostok, Russia*, pages 1–10, 2003.

[11] International Electrotechnical Commission. IEC 60850 International Standard: Railway Applications - Supply Voltages of Traction Systems, 2014.

[12] IEEE Industry Applications Society. IEEE Recommended Practice for 1 kV to 35 kV Medium-Voltage DC Power Systems on Ships. Technical Report November, 2010.

[13] Fred Wang, Yunqing Pei, Dushan Boroyevich, Rolando Burgos, and Khai Ngo. AC vs. DC distribution for Off-Shore Power Delivery. In *IECON Proceedings (Industrial Electronics Conference)*, pages 2113–2118, 2008.

[14] F. H. Kreuger. *Industrial High DC Voltage*. 1995.

[15] Florian Mura and Rik W De Doncker. Preparation of a Medium-Voltage DC Grid Demonstration Project. *E.ON Energy Research Center Series*, 4(1):1–32, 2012.

[16] Xiang Zhang and Steven Pekarek. A Coupled Thermal/Electric Circuit Model for Design of MVDC Ship Cables. In *2017 IEEE Electric Ship Technologies Symposium, ESTS 2017*, pages 71–78, 2017.

[17] Marco Stieneker. *Analysis of Medium-Voltage Direct-Current Collector Grids in Offshore Wind Parks*. 2017.

[18] Siemens. MVDC - Managing the future grid, 2017.

[19] Forschungscampus FEN. First Medium-Voltage DC Grid in Aachen, 2018.

[20] F. Mura and Rik W. De Doncker. Design Aspects of a Medium-Voltage Direct Current (MVDC) Grid for a University Campus. In *8th International Conference on Power Electronics - ECCE Asia: "Green World with Power Electronics", ICPE 2011-ECCE Asia*, number Mvdc, pages 2359–2366, 2011.

[21] Mehdi Monadi, Cosmin Koch-Ciobotaru, Alvaro Luna, Jose Ignacio Candela, and Pedro Rodriguez. Multi-Terminal Medium Voltage DC Grids Fault Location and Isolation. *IET Generation, Transmission & Distribution*, 10(14):3517–3528, 2016.

[22] Uzair Javaid, Drazen Dujic, and Wim Van Der Merwe. MVDC Marine Electrical Distribution: Are We Ready? In *IECON 2015 - 41st Annual Conference of the IEEE Industrial Electronics Society*, pages 823–828, 2015.

[23] Gregory F. Reed, Brandon M. Grainger, Adam R. Sparacino, and Zhi-Hong Mao. Ship to Grid. *IEEE Power and Energy Magazine*, (november/december):70–79, 2012.

[24] Andreas Giannakis and Dimosthenis Peftitsis. MVDC Distribution Grids and Potential Applications : Future Trends and Protection Challenges. In *2018 20th European Conference on Power Electronics and Applications*, pages 1–11, 2018.

[25] Heather Pugliese and Michael Von Kannewurff. Discovering DC: A Primer on DC Circuit Breakers, Their Advantages, and Design. *IEEE Industry Applications Magazine*, 19(5):22–28, 2013.

[26] Neal R. Butler, Richard C. Myer, James E. Petry, Simon S. Normand, D. M. Robinson, Marcel P.J. Gaudreau, and Wayne J. Beckman. Undersea MVDC Power Distribution. *Proceedings of the 2010 IEEE International Power Modulator and High Voltage Conference, IPMHVC 2010*, pages 294–297, 2010.

[27] Ranjan K. Gupta and Kevin G Collins. System for Operation of Photovoltaic Power Plant and DC Power Collection Within, 2015.

[28] Frede. Blaabjerg and Ke. Ma. Wind Energy Systems. In *Proceedings of the IEEE*, volume 105, pages 735–762, 2017.

[29] Mikel De Prada Gil, J. L. Domínguez-García, F. Díaz-González, M. Aragüés-Peñalba, and Oriol Gomis-Bellmunt. Feasibility analysis of offshore wind power plants with DC collectiongrid. *Renewable Energy*, 78:467–477, 2015.

[30] Wu Chen, Alex Q Huang, Chushan Li, Gangyao Wang, and Wei Gu. Analysis and Comparison of Medium Voltage High Power DC / DC Converters for Offshore Wind Energy Systems. 28(4):2014–2023, 2014.

[31] By Ram Adapa. High-Wire Act. *IEEE Power & Energy Magazine*, november/d:18–29, 2012.

[32] Oluwafemi E. Oni, Innocent E. Davidson, and Kamati N.I. Mbangula. A Review of LCC-HVDC and VSC-HVDC Technologies and Applications. *EEEIC 2016 - International Conference on Environment and Electrical Engineering*, (September), 2016.

[33] Jin Yang, John E. Fletcher, and John O'Reilly. Short-Circuit and Ground Fault Analyses and Location in VSC-based DC Network Cables. *IEEE Transactions on Industrial Electronics*, 59(10):3827–3837, 2012.

[34] Alstom Grid. *Network Protection & Automation*. May 2011 edition, 2011.

[35] Rich Schmerda, Rob Cuzner, Rodney Clark, Dan Nowak, and Steve Bunzel. Shipboard Solid-State Protection: Overview and Applications. *IEEE Electrification Magazine*, 1(1):32–39, 2013.

[36] Wen Shan Tan, Mohammad Yusri Hassan, Md Shah Majid, and Hasimah Abdul Rahman. Optimal Distributed Renewable Generation Planning: A Review of Different Approaches. *Renewable and Sustainable Energy Reviews*, 18(February):626–645, 2013.

[37] Mustafa Farhadi and Osama A. Mohammed. Protection of Multi-Terminal and Distributed DC Systems: Design Challenges and Techniques. *Electric Power Systems Research*, 143:715–727, 2017.

[38] Dragan Jovcic and Bin Wu. Fast Fault Current Interruption on High-Power DC Networks. In *IEEE PES General Meeting, PES 2010*, pages 4–9, 2010.

[39] Robert M. Cuzner and Vikas Singh. Future Shipboard MVDC System Protection Requirements and Solid-State Protective Device Topological Tradeoffs. *IEEE Journal of Emerging and Selected Topics in Power Electronics*, 5(1):244–259, 2017.

[40] X. Pei, O. Cwikowski, D. S. Vilchis-Rodriguez, M. Barnes, A. C. Smith, and R. Shuttleworth. A Review of Technologies for MVDC Circuit Breakers. *IECON Proceedings (Industrial Electronics Conference)*, 0:3799–3805, 2016.

[41] Andreas Giannakis and Dimosthenis Peftitsis. Design Considerations of Power Semiconductor Devices Employed in VSCs Under Short-Circuit Fault Conditions in MVDC Distribution Grids.

[42] Magnus Callavik, Anders Blomberg, Jrgen Häfner, and Bjrn Jacobson. The Hybrid HVDC Breaker An Innovation Breakthrough Enabling Reliable HVDC Grids. Technical report, 2012.

[43] Ming Chen, Yuming Zhao, Xiaolin Li, Shukai Xu, Weimin Sun, Tong Zhu, Rong Zeng, Zhenyu Chen, and Zhanqing Yu. Development of Topology and Power Electronic Devices for Solid-State Circuit Breakers. *Proceedings - 2013 2nd International Symposium on Instrumentation and Measurement, Sensor Network and Automation, IMSNA 2013*, pages 190–193, 2013.

[44] Anshuman Shukla and Georgios D. Demetriades. A Survey on Hybrid Circuit-Breaker Topologies. *IEEE Transactions on Power Delivery*, 30(2):627–641, 2015.

[45] Andreas Huerner, Tobias Erlbacher, Anton J. Bauer, and Lothar Frey. Monolithically Integrated Solid-State-Circuit-Breaker for High Power Applications. *Materials Science Forum*, 897:661–664, 5 2017.

[46] Oleg Vodyakho, Michael Steurer, Dominik Neumayr, C.S. Edrington, G. Karady, and Subhashish Bhattacharya. Solid-State Fault Isolation Devices: Application to Future Power Electronics-Based Distribution Systems. In *2011 IEEE Applied Power Electronics Conference and Exposition*, pages 113–118. APEC, 2011.

[47] Volker Staudt, Roman Bartelt, and Carsten Heising. Short-Circuit Protection Issues in DC Ship Grids. *2013 IEEE Electric Ship Technologies Symposium, ESTS 2013*, pages 475–479, 2013.

[48] Chang Peng, Xiaoqing Song, Mohammad Ali Rezaei, Xing Huang, Chris Widener, Alex Q. Huang, and Michael Steurer. Development of Medium Voltage Solid-State Fault Isolation Devices For Ultra-Fast Protection of Distribution Systems. In *IECON Proceedings (Industrial Electronics Conference)*, pages 5169–5176. IEEE, 2014.

[49] Haijin Li, Jianan Zhou, Zhaoyu Liu, and Dehong Xu. Solid State DC Circuit Breaker for Super Uninterruptible Power Supply. *Proceedings - 2014 International Power Electronics and Application Conference and Exposition, IEEE PEAC 2014*, pages 1230–1235, 2014.

[50] M. Kempkes, I. Roth, and M. Gaudreau. Solid-State Circuit Breakers for Medium Voltage DC Power. *2011 IEEE Electric Ship Technologies Symposium, ESTS 2011*, pages 254–257, 2011.

[51] Sondre Johan Kjellin Berg. Solid State Circuit Breakers In Medium Voltage Direct Current Systems, 2018.

[52] Kenichiro Sano and Masahiro Takasaki. A Surgeless Solid-State DC Circuit Breaker for Voltage-Source-Converter-Based HVDC Systems. *IEEE Transactions on Industry Applications*, 50(4):2690–2699, 2014.

[53] Slobodan Krstic, Edward L. Wellner, Ashish R. Bendre, and Boris Semenov. Circuit Breaker Technologies for Advansed Ship Power Systems. In *2007 IEEE Electric Ship Technologies Symposium*, pages 201–208, 2007.

[54] M. Kohlmann, T. Küper, V. Staudt, and A. Steimel. Combined Solid-State AC/DC Switch for Laboratory Applications. *PCIM Europe Conference Proceedings*, (May):1515–1521, 2014.

[55] Mu Jian-Guo, Wang Li, and Hu Jie. Research on Main Circuit Topology for a Novel DC Solid-State Circuit Breaker. *Proceedings of the 2010 5th IEEE Conference on Industrial Electronics and Applications, ICIEA 2010*, pages 926–930, 2010.

[56] Jin Young Kim, Seung Soo Choi, Seung Min Song, and In Dong Kim. New DC Solid State Circuit Breaker with Reclosing and Rebreaking Capabilities. *2016 IEEE 8th International Power Electronics and Motion Control Conference, IPEMC-ECCE Asia 2016*, pages 3554–3558, 2016.

[57] Keith A. Corzine. A New-Coupled-Inductor Circuit Breaker for DC Applications. *IEEE Transactions on Power Electronics*, 32(2):1411–1418, 2017.

[58] Keith A. Corzine and Robert W. Ashton. Structure and Analysis of the Z-Source MVDC Breaker. *2011 IEEE Electric Ship Technologies Symposium, ESTS 2011*, pages 334–338, 2011.

[59] Keith A. Corzine and Robert W. Ashton. A New Z-source DC Circuit Breaker. *IEEE Transactions on Power Electronics*, 27(6):2796–2804, 2012.

[60] Chen Yuan, Mohammed A. Haj-Ahmed, and Mahesh S. Illindala. Protection Strategies for Medium-Voltage Direct-Current Microgrid at a Remote Area Mine Site. *IEEE Transactions on Industry Applications*, 51(4):2846–2853, 2015.

[61] Marco Stieneker and Rik W. De Doncker. Medium-Voltage DC Distribution Grids in Urban Areas. *2016 IEEE 7th International Symposium on Power Electronics for Distributed Generation Systems, PEDG 2016*, pages 0–6, 2016.

[62] Gregory F. Reed, Brandon M. Grainger, Matthew J. Korytowski, and Emmanuel J. Taylor. Modeling, Analysis, and Validation of a Preliminary Design for a 20 kV Medium Voltage DC Substation. *IEEE 2011 EnergyTech, ENERGYTECH 2011*, pages 1–8, 2011.

[63] Graeme Bathurst, George Hwang, and Lalit Tejwani. MVDC - The New Technology for Distribution Networks. *11th IET International Conference on AC and DC Power Transmission*, (Dc):1–5, 2015.

[64] P Steimer, O Apeldoorn, and E Carroll. IGCT Devices-Applications and Future Opportunities. *Power Engineering Society Summer Meeting, 2000. IEEE*, 2(February 2000):1223–1228, 2000.

[65] Rafa Kopacz, Dimosthenis Peftitsis, and Jacek Rabkowski. Experimental Study on Fast-Switching Series-Connected SiC MOSFETs. In *2017 19th European Conference on Power Electronics and Applications (EPE'17 ECCE Europe)*, pages 1–10, 2017.

[66] Dimosthenis Peftitsis, Jacek Rabkowski, Hans-Peter Nee, and Tore Undeland. Challenges on Drive Circuit Design for Series-Connected SiC Power Transistors. In *Material Science Forum*, pages 655–660, 2017.

[67] Bin Zhang. Development of the Advanced Emitter Turn-Off (ETO) Thyristor. 2005.

[68] ABB. StatPak IGBT Module - 5SNA 3000K452300 Datasheet, 2017.

[69] Robin Simpson, Ashley Plumpton, Michael Varley, Charles Tonner, Paul Taylor, and Xiaoping Dai. Press-pack IGBTs for HVDC and FACTs. *CSEE Journal of Power and Energy Systems*, 3(3):302–310, 2017.

[70] Soonwook Hong and Yong-Geun Lee. Active Gate Control Strategy of Series Connected IGBTs for High Power PWM Inverter. In *IEEE 1999 International Conference on Power Electronics and Drive Systems*, pages 646–652, 1999.

[71] Igor Baraia, Jon Andoni Barrena, Gonzalo Abad, Jos Mara Canales Segade, and Unai Iraola. An Experimentally Verified Active Gate Control Method for the Series Connection of IGBT/Diodes. *IEEE Transactions on Power Electronics*, 27(2):1025–1038, 2012.

[72] Xigen Zhou, Zhenxue Xu, Alex Q Huang, and Dushan Boroyevich. Comparison of High Power IGBT, IGCT and ETO for Pulse Applications. In *Annual Power Electronics Seminar*, pages 506–510, 2002.

[73] William McMurray. Efficient Snubbers for Voltage-Source GTO Inverters. *IEEE Transactions on Power Electronics*, PE-2(3):264–272, 1987.

[74] ABB. Asymmetric Integrated Gate-Commutated Thyristor - 5SHY 55L4500 Datasheet, 2013.

[75] X Wang, A Caiafa, J Hudgins, and E Santi. Temperature Effects on IGCT Performance. *Industry Applications Conference, 2003, 38th IAS Annual Meeting. Conference Record of the*, 00(C):0–5, 2003.

[76] P. K. Steimer, H. J. Grüning, and J. Werninger. The IGCT - The Key Technology for Low Cost, High Releable High Power Converters with Series Connected Turn-Off Devices. *European Power Electronics and Drives (EPE)*, (September):8–10, 1997.

[77] Muhammad H. Rashid. *Power Electronics Handbook*. 2018.

[78] P. K. Steimer, H. E. Gruning, J. Werninger, E. Carroll, S. Klaka, and S. Linder. IGCT: A New Emerging Technology for High Power, Low Cost Inverters. In *IAS '97. Conference Record of the 1997 IEEE Industry Applications Conference Thirty-Second IAS Annual Meeting*, pages 1592–1599, 1997.

[79] Horst Grüning. IGCT Technology: A Quantum Leap for High-power Converters, 2017.

[80] Umamaheswara Vemulapati, Munaf Rahimo, Tobias Wikström, and Thomas Stiasny. Recent Advancements in IGCT Technologies for High-Power Electronics Applications. In *EPE 2005 Conference*, 2005.

[81] Francesco Agostini, Umamaheswara Vemulapati, Daniele Torresin, Martin Arnold, Munaf Rahimo, Antonello Antoniazzi, Luca Raciti, Davide Pessina, and Harish Suryanarayana. 1MW Bi-Directional DC Solid State Circuit Breaker Based on Air Cooled Reverse Blocking-IGCT. In *2015 IEEE Electric Ship Technologies Symposium, ESTS 2015*, pages 287–292. IEEE, 2015.

[82] Martin Arnold, Antonello Antoniazzi, Munaf Rahimo, Davide Pessina, and Umamaheswara Vemulapati. Reverse Blocking IGCT Optimised for 1 kV DC bi-Directional Solid State Circuit Breaker. *IET Power Electronics*, 8(12):2308–2314, 2015.

[83] Eric Carroll, Bjoern Oedegard, Thomas Stiasny, and Marco Rossinelli. Application Specific IGCTs. *ICPE*, 2001(October):1–5, 2001.

[84] M Rahimo, A Kopta, U Schlapbach, J Vobecky, R Schnell, and S Klaka. The Bi-mode Insulated Gate Transistor (BIGT): A Potential Technology for Higher Power Applications. In *2009 21st International Symposium on Power Semiconductor Devices & IC's*, pages 283–286. IEEE, 2009.

[85] M Rahimo and Liutauras Storasta. Optimization and Advantages of the Bi-Mode Insulated Gate Transistor. *Facta Universitatis - Electronics and Energetics*, 28(3):383–391, 2015.

[86] L. Storasta, A. Kopta, and M. Rahimo. A Comparison of Charge Dynamics in the Reverse-Conducting RC IGBT and Bi-mode Insulated Gate Transistor BiGT. In *2010 22nd International Symposium on Power Semiconductor Devices*, pages 391–394, 2010.

[87] A. Kopta and M. Rahimo. The Field Charge Extraction (FCE) Diode A Novel Technology for Soft Recovery High Voltage Diodes. In *Proceedings. ISPSD '05. The 17th International Symposium on Power Semiconductor Devices and ICs, 2005.*, pages 1–4. IEEE, 2005.

[88] Umamaheswara Vemulapati, Marco Bellini, Martin Arnold, Munaf Rahimo, and Thomas Stiasny. The concept of bi-mode gate commutated thyristor: A new type of reverse conducting IGCT. In *Proceedings of the International Symposium on Power Semiconductor Devices and ICs*, number June, pages 29–32. IEEE, 2012.

[89] N. Lophitis, M. Antoniou, U. Vemulapati, M. Arnold, I. Nistor, J. Vobecky, M. Rahimo, and F. Udrea. New Bi-Mode Gate-Commutated Thyristor Design Concept for High-Current Controllability and Low ON-State Voltage Drop. *IEEE Electron Device Letters*, 37(4):467–470, 2016.

[90] Yuxin Li, Alex Q Huang, and Fred C Lee. Introducing the Emitter Turn-off Thyristor (ETO). In *Conference Record of 1998 IEEE Industry Applications Conference. Thirty-Third IAS Annual Meeting*, pages 860–864, 1998.

[91] Zhenxue Xu, Bin Zhang, S. Sirisukprasert, Xigen Zhou, and A.Q. Huang. The Emitter Turn-Off Thyristor-Based DC Circuit Breaker. In *2002 IEEE Power Engineering Society Winter Meeting. Conference Proceedings (Cat. No.02CH37309)*, pages 288–293. IEEE, 2002.

[92] B. Chen, A.Q. Huang, M. Baran, C. Han, and W. Song. Operation Characteristics of Emitter Turn-Off Thyristor (ETO) for Solid-State Circuit Breaker and Fault Current Limiter. *Twenty-First Annual IEEE Applied Power Electronics Conference and Exposition, 2006. APEC '06.*, pages 174–178, 2006.

[93] Liqi Zhang, Richard Woodley, Xiaoqing Song, Soumik Sen, Xin Zhao, and Alex Q. Huang. High Current Medium Voltage Solid State Circuit Breaker Using Paralleled 15kV SiC ETO. *Conference Proceedings - IEEE Applied Power Electronics Conference and Exposition - APEC*, 2018-March(March):1706–1709, 2018.

[94] John Waldron and Silicon Power Corporation. Low-loss , Fast-acting Solid State AC / DC Breaker. In *PCIM Asia 2016 - International Exhibition and Conference for Power Electronics, Intelligent Motion, Renewable Energy and Energy Management*, pages 192–197, 2016.

[95] Q. Zhang, A. Agarwal, C. Capell, L. Cheng, M. O'Loughlin, A. Burk, J. Palmour, Victor Temple, Aderinto Ogunniyi, Heather O'Brien, and Charles J. Scozzie. SiC Super GTO Thyristor Technology Development: Present Status and Future Perspective. *Digest of Technical Papers - IEEE International Pulsed Power Conference*, pages 1530–1535, 2011.

[96] Vic Temple. Super GTOs Push the Limits of Thyristor Physics. In *IEEE Power Electronics Specialists Conference*, pages 604–610, 2004.

[97] Timothy E Griffin. Super Gate Turn-Off Thyristor. Technical Report August, Army Research Laboratory, 2006.

[98] Vikas Singh. *Solid State Protective Device Topological Trade-offs for Mvdc Systems*. PhD thesis, University of Wisconsin-Milwaukee, 2016.

[99] Yusi Liu, Chris Farnell, Hao Zhang, Andrs Escobar-Mejía, H. Alan Mantooth, Juan Carlos Balda, and Simon S. Ang. A Silicon Carbide Fault Current Limiter for Distribution Systems. In *2014 IEEE Energy Conversion Congress and Exposition, ECCE 2014*, pages 4972–4977, 2014.

[100] Chunyang Gu, Pat Wheeler, Alberto Castellazzi, Alan J. Watson, and Francis Effah. Semiconductor Devices in Solid-State/Hybrid Circuit Breakers: Current Status and Future Trends. *Energies*, 10(4), 2017.

[101] Diane Perle Sadik, Juan Colmenares, Georg Tolstoy, Dimosthenis Peftitsis, Mietek Bakowski, Jacek Rabkowski, and Hans Peter Nee. Short-Circuit Protection Circuits for Silicon-Carbide Power Transistors. *IEEE Transactions on Industrial Electronics*, 63(4):1995–2004, 2016.

[102] Z. John Shen, Gourab Sabui, Zhenyu Miao, and Zhikang Shuai. Wide-Bandgap Solid-State Circuit Breakers for DC Power Systems: Device and Circuit Considerations. *IEEE Transactions on Electron Devices*, 62(2):294–300, 2015.

[103] Z. John Shen, Zhenyu Miao, and Aref Moradkhani Roshandeh. Solid State Circuit Breakers for DC Microgrids: Current Status and Future Trends. *2015 IEEE 1st International Conference on Direct Current Microgrids, ICDCM 2015*, pages 228–233, 2015.

[104] Roger Allan. SiC and GaN vs. IGBTs: The Imminent Tug of War for Supremacy. *Power Electronics*, (July):2–3, 2017.

[105] M Janicki and A Napieralski. Modelling Electronic Circuit Radiation Cooling Using Analytical Thermal Model. *Microelectronics Journal*, 31(9):781–785, 2000.

[106] S Narumanchi, M Mihalic, K Kelly, and G Eesley. Thermal Interface Materials for Power Electronics Applications. In *Itherm*, 2008.

[107] Priyanka Jaiswal and C K Dwivedi. Thermal Interface Materials used for Improving the Efficiency and Power Handling Capability of Electronic Devices: A Review. *International Journal of Innovative Technology & Creative Engineering*, 1(5):2045–2053, 2011.

[108] Rui Wu, Huai Wang, Ke Ma, Pramod Ghimire, Francesco Iannuzzo, and Frede Blaabjerg. A Temperature-Dependent Thermal Model of IGBT Modules Suitable for Circuit-Level Simulations. In *2014 IEEE Energy Conversion Congress and Exposition (ECCE)*, pages 2901–2908, 2014.

[109] Sukhvinder S. Kang. Advanced Cooling for Power Electronics. In *International Conference on Integrated Power Electronics Systems*, 2012.

[110] ABB. 5SYA 2036-04: Mechanical Clamping of Press-Pack High Power Semiconductors, 2016.

[111] Shusheng Wang, Zhiquan Song, Peng Fu, Kun Wang, Xuesong Xu, Wei Tong, and Zhongma Wang. Thermal Analysis of Water-cooled Heat Sink for Solid-State Circuit Breaker Based on IGCTs in Parallel. *IEEE Transactions on Components, Packaging and Manufacturing Technology*, 9(3):483–488, 2018.

[112] Ned Mohan, Tore M. Undeland, and William P. Robbins. *Power Electronics*. 2012.

[113] AMS Technologies. Heat Sinks and Water Coolers, 2013.

[114] IXYS UK Westcode Ltd. Heatsink Type XSFTCxxxxAN, 2014.

[115] Jian Zhang and Donglai Zhang. The Calculation of Thermal Resistance for Forced Air Cooling. In *International Symposium on Material, Energy and Environment Engineering*, pages 622–625, 2015.

[116] C Gillot, C Schaeffer, R Perret, C Massit, and L Meysenc. Double-sided Cooling for High Power IGBT Modules using Flip Chip Technology. *Power*, pages 3016–3020, 2000.

[117] Keiji Wada, Jumpei Koyama, Kazuto Takao, Takeo Kanai, and Hiromichi Oohashi. Thermal Analysis for Hybrid Pair Module of Si-IEGT and SiC-PiN Diode. *2010 International Power Electronics Conference - ECCE Asia -, IPEC 2010*, pages 2135–2140, 2010.

[118] Laurent Dupont and Yvan Avenas. Evaluation of Thermo-Sensitive Electrical Parameters Based on the Forward Voltage for On-Line Chip Temperature Measurements of IGBT Devices. *2014 IEEE Energy Conversion Congress and Exposition (ECCE)*, pages 4028–4035, 2014.

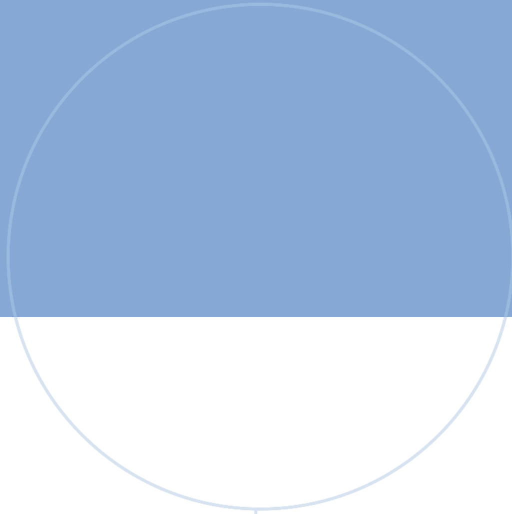
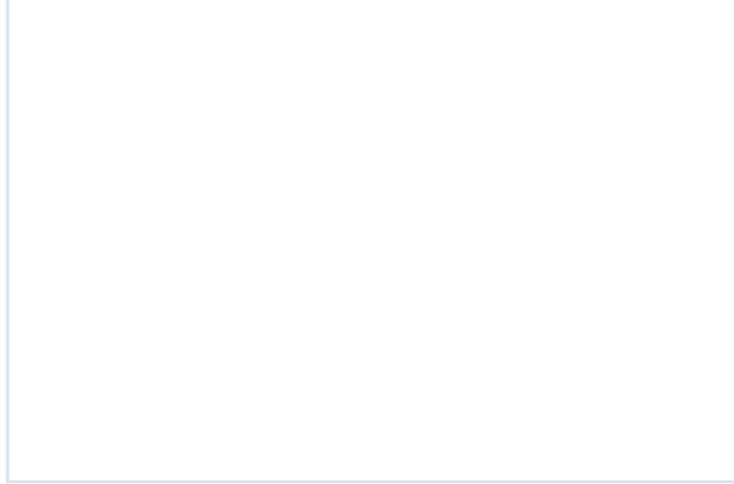

NTNU
Norwegian University of
Science and Technology